



NTNU – Trondheim
Norwegian University of
Science and Technology

Reliability-based design optimization with Cross-Entropy method

Hiruy Ghidey

Geotechnics and Geohazards

Submission date: June 2015

Supervisor: Gudmund Reidar Eiksund, BAT

Norwegian University of Science and Technology
Department of Civil and Transport Engineering

Thesis Title:				
<i>Reliability-based design optimization with Cross-Entropy method</i>	Date: June 9 th , 2015			
	Number of pages (incl. appendices): 85			
Name: <i>Hiruy Ghidey Hishe</i>	Master Thesis	X	Semester Project	
Professor in charge/supervisor: <i>Professor Gudmund Eiksund</i>				
Co-supervisor: <i>Ivan Depina, PhD student</i>				
<p>Abstract:</p> <p>Implementation of the Cross-entropy (CE) method to solve reliability-based design optimization (RBDO) problems was investigated. The emphasis of this implementation method was to solve independently both the reliability and optimization sub-problems within the RBDO problem; therefore, the main aim of this study was to evaluate the performance of the Cross-entropy method in terms of efficiency and accuracy to solve RBDO problems.</p> <p>A numerical approach was followed in which the implementation and preparation of the CE algorithm for the numerical modelling and simulations were performed on the high level language, MATLAB (R2014a and R2013b).</p> <p>The CE algorithm was prepared for reliability analysis and further developed to account for optimization problems. The CE method was initially validated on an academic RBDO problem within an analytical solution and the necessary parameter study of the CE algorithm was conducted. In the meantime, the efficiency and accuracy of the CE method were evaluated in comparison with existing reliability and optimization methods. Finally, the developed algorithm was examined and evaluated on an RBDO problem of a practical design of a laterally loaded monopile foundation for offshore wind turbines.</p> <p>The CE method showed efficient performance on RBDO problems. Moreover, the method gave both efficient (less simulation time) and accurate results by comparing it to analytical solutions and existing reliability as well as optimization methods.</p> <p>Some recommendations and future works were also pointed out and discussed.</p>				

Keywords:

1.Cross-entropy
2.Reliability-based design optimization (RBDO)
3.Algorithm
4.Efficiency
5.MATLAB

MASTER THESIS

SPRING 2015

For

HIRUY GHIDEY HISHE

Reliability-based design optimization with Cross-Entropy method**BACKGROUND**

Facilities such as bridges, power plants, dams and offshore platforms require high construction cost. Failure of such structures could result in public safety issues as well as economy and environmental consequences. Reducing the probability of failure and cost of construction of these structures is an important part of engineering design to keep the structures safe (reliable) with seeking minimum (optimum) construction cost.

Different design approaches are currently in use for safe design of structures. For simple structures and less uncertainties in the input parameters (e.g. material properties, loads, etc.), a direct or deterministic approach using a factor of safety is implemented due to ease and time saving design. Alternative to the factor of safety design is a probabilistic framework known as Reliability-based design which quantifies uncertainties in design parameters to produce a design with acceptably small failure probability.

Extension of a Reliability-based design approach, known as Reliability-based design optimization (RBDO) is considered in this study as a promising methodology for design in geotechnical engineering. An advantage of the RBDO approach is that it allows for determining the best design solution while explicitly considering the effects of uncertainties in engineering design.

Various algorithms were developed to solve reliability and optimization sub-problems within the RBDO problem. The main shortcoming of existing RBDO algorithms is that they are computationally demanding, because both reliability and optimization algorithms can require large number of simulations of computationally complex models simulating the response of a structure or an engineering system.

TASK

The main task for this thesis is to implement a method known as Cross-entropy to solve independently reliability and optimization sub-problems within the RBDO problem. The performance of the Cross-entropy method is examined on an RBDO problem with an analytical solution and a practical problem of a monopile foundation for offshore wind turbine.

Task description

The application of the Cross-entropy method to the RBDO problem is advantageous due to the flexibility of the Cross-entropy method to deal with both reliability and optimization problems. The resulting RBDO algorithm is a double-loop algorithm with the reliability problem solved within the optimization algorithm. The performance of the Cross-entropy method with respect to accuracy and efficiency on both reliability and optimization problems is compared to several commonly used methods. Due to the focus on geotechnical applications where high dimensional reliability problem are common, special attention was given to the limitations of the Cross-entropy method with respect to the dimensionality of reliability problems.

Objective and purpose

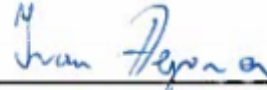
The objective of this thesis is to demonstrate the advantages of the RBDO formulations in an engineering design and utilize the flexibility of the Cross-entropy method to deal with the reliability and optimization sub-problems within the RBDO problem.

Subtasks and research questions

- Literature study on the existing reliability and optimization algorithms.
- Implementation and validation of the Cross-entropy method for reliability and optimization problems.
- Implementation of the Cross-entropy method for RBDO.
- Validation of the Cross-entropy method on an RBDO problem with an analytical solution, and a practical RBDO problem of a monopile foundation for offshore wind turbine.



Prof. Gudmund Eiksund
NTNU



Ivan Depina (MSc)
NTNU

Preface

This master thesis was undertaken at the Geotechnical Division of Civil and Transport Engineering Department, Norwegian University of Science and Technology (NTNU) in partial fulfillment of the requirement for MSc in Geotechnics and Geohazards. It was carried out in the spring semester of 2015.

The idea for this master thesis was initiated by Ivan Depina, PhD student at NTNU, with the aim of implementing and utilizing the flexibility of the Cross-entropy method to deal with the reliability and optimization sub-problems within the reliability-based design optimization (RBDO).

Trondheim, Norway



Hiruy Ghidey Hishe

June, 2015

Acknowledgment

First, I would like to thank God for his endless blessings that gave me strength and patience all the way in my life.

It is with a great pleasure I thank and appreciate my co-supervisor, Ivan Depina (PhD student at NTNU), for his valuable suggestions, constructive criticism, and continuous and motivating support. All the discussions and comments were very constructive not only for this master thesis but for future research and investigations.

I would also like to thank my supervisor, Prof. Gudmund Eiksund, for his support when I needed assistance and critical comments during the progress of the thesis.

I am highly grateful for the Norwegian University of Science and Technology NTNU and the Norwegian State Educational Loan Fund for giving me the opportunity to study my master degree and financing for my stay here in Norway.

It is with a great pleasure I would like to dedicate this master thesis to my dear parents-Ghidey Hishe and Letay Mehari for their unconditional love and belief in me. My thanks also go to my brother-Kibreab (PhD) and sisters-Liwam and Lemlem. The encouragement and support from my friends both from Ethiopia and Norway is priceless. My special thanks go to Xiang, Antonios, Cecilie, Suresh, Ashenafi, Bereketiab, Kominist, Berhane and Tesfaye for making my stay in Norway memorable. Last but not least, my special thanks goes to Conor Waller for proofreading the thesis.

Hiruy Ghidey

Trondheim, June 2015

Contents

Abstract	iii
Preface	vii
Acknowledgement.....	ix
Contents.....	xi
List of Figures	xiii
List of Tables.....	xiv
List of Symbols	xv
1. Introduction	1
1.1 Background.....	1
1.2 Objective of study.....	2
1.3 Study Approach	2
1.4 Scope of the Thesis.....	3
1.5 Limitation	3
1.6 Structure of the Thesis	3
2. Literature Review	5
2.1 Introduction	5
2.2 Reliability and Reliability Analysis Methods.....	6
2.2.1 Sampling Methods.....	7
2.3 Reliability Methods which apply optimization methods.....	14
2.3.1 Justification of Reliability Methods using a Non-linear Example	16
2.4 Reliability-Base design Optimization (RBDO).....	19
3. Cross Entropy Algorithm for Reliability Analysis and Optimization	23
3.1 Introduction	23
3.2 Cross-Entropy for Rare-event Probability Estimation.....	24
3.2.1 Kullback-Leibler distance	25
3.3 Cross-Entropy Method for Optimization.....	28
4. CE-RBDO Validation on an academic Example	33
4.1 Introduction	33
4.2 Problem Definition	33
4.3 Reliability Analysis using CE algorithm	34
4.3.1 One-dimensional problem (1D)	35
4.3.2 Two-dimensional (2D) and higher dimensional Problems	35

4.3.3	Comparison of the CE algorithm results with existing methods.....	41
4.3.4	Discussion and Summary on reliability analysis.....	41
4.4	Optimization Analysis using CE method	42
4.4.1	Results for Two-dimensional (n=2 and d=2)	44
4.4.2	Results for high dimensions (n>2 and d>2)	47
4.4.3	Discussion and Summary on optimization analysis	48
5.	Reliability-Based Design of a Monopile Foundation.....	49
5.1	Introduction	49
5.2	Soil variability	52
5.3	Lateral load	55
5.4	Pile geometry.....	55
5.5	Reliability analysis (Estimation of P_f for the monopile foundation).....	55
5.5.1	Preparation of the Algorithm for Reliability	56
5.6	Optimization Problem.....	57
5.6.1	Preparation of the Algorithm for Optimization.....	58
5.7	Results and Discussion	59
5.7.1	Reliability Analysis of a monopile foundation	59
5.7.2	Results for the Optimization Problem.....	62
6.	Summary and Conclusions.....	65
6.1	Introduction	65
6.2	Summary of Important findings	65
6.2.1	Summary on reliability analysis and findings	66
6.2.2	Summary on Optimization analysis and findings	67
6.3	Conclusion, Recommendations and Future works	68
6.3.1	Conclusion and Recommendations	68
6.3.2	Future works.....	69
Reference	70

List of Figures

Figure 2.1 Reliability analysis between θ_1 and θ_2 on $h(\boldsymbol{\theta})$ (Adopted from (Depina, 2014)).....	7
Figure 2.2 Importance distribution illustration (Adopted from (Gu, 2014)).....	11
Figure 2.3 Approximation of non-linear $g(\boldsymbol{\theta})$ using FORM and SORM (Depina, 2014)	16
Figure 2.4 Distribution of variable vectors for $N=1000$ (normal distributions).....	17
Figure 2.5 Subset simulation result for $N=10,000$ samples	18
Figure 2.6 Cooling process of particles to yield low energy state (Depina, 2014)	21
Figure 3.1 Development of the Cross-entropy method for reliability analysis.....	27
Figure 3.2 Illustration of the CE optimization method	30
Figure 4.1 Plot for $\rho=0.01$ (left) and $\rho=0.05$ (right) with $N=800$	38
Figure 4.2 Plot for $\rho=0.1$ (left) and $\rho=0.4$ (right) with $N=800$	38
Figure 4.3 Illustration of 2D (left) and 3D (right) view for convergence of $g(\boldsymbol{\theta})$	39
Figure 4.4 Estimation of P_f or β for $n=50$, $d=50$ for $\rho=0.3$ and $\rho=0.4$	40
Figure 4.5 In-plot of Cost over e^{t_1} and e^{t_2}	46
Figure 4.6 Contour plotting of $\ln(C)$ over t_1 and t_2	46
Figure 4.7 Estimation of C_{\min} and respective design points from simulated annealing.....	47
Figure 5.1 Winkler approach with the pile modelled as an elastic beam supported by nonlinear and coupled springs (Bekken, 2009)	50
Figure 5.2 Shear strength and realization along the depth	53
Figure 5.3 Gumbel distribution of lateral load, H	55
Figure 5.4 Evolution of D to optimum value, $D=5.15\text{m}$, after four iterations	63
Figure 5.5 Evolution of L to optimum value, $L=30\text{m}$, after four iterations	63
Figure 5.6 Evolution of w to optimum value, $w=0.045\text{m}$, after four iterations.....	64
Figure 5.7 Evolution of cost to optimum value, $C_{\min}=3.2490\text{e}+05\text{€}$, after four iterations.....	64

List of Tables

Table 2-1 Estimated P_f values using FOSM, FORM, MC, IM and Subset simulation for different sample sizes, N	17
Table 4-1 Results of the MC, IM and CE and analytical solution	35
Table 4-2 Estimation of P_f for $n=2$, $d=2$ and $\rho =0.1$ with variable α_r , β_r and N	37
Table 4-3 Estimation for $(n=5, d=5)$, $(n=10, d=10)$ and $(n=20, d=20)$	40
Table 4-4 Estimation of P_f for $n= 60$ and $d=60$	40
Table 4-5 Comparison of the CE method with other existing methods	41
Table 4-6 Comparison of Algorithm solution with Analytical solution	45
Table 4-7 High dimensional optimization problems compared with the analytical solution...	47
Table 5-1 Representative of k_s for overconsolidated clay (API, 2000).....	51
Table 5-2 Representative of ε_{50} for overconsolidated clay (API, 2000).....	51
Table 5-3 Estimation of P_f for the different combinations of α_r and β_r	59
Table 5-4 Effect of ρ on estimate of P_f	60
Table 5-5 Comparison of CE with SS for monopile foundation, Case-1	60
Table 5-6 Summary of comparison between CE and SS methods.....	61
Table 5-7 Comparison with SS for random pile dimensions (D , w and L).....	61
Table 5-8 Pile parameters D , w , L for initial cost C_i and minimum final cost C_{\min}	62
Table 5-9 Convergence of D , w and L as a result of small standards deviation	62

List of Symbols

Roman Letters

C	Positive numbers	P_f	Probability of failure
C	Cost (€)	$P(F_i F_{i-1})$	Conditional probability
\mathbf{C}	Correlation matrix	p_u	Ultimate soil resistance per unit length (kN/m)
D	Pile diameter (m)	\mathbf{R}	Space
dz	Infinitesimal small element	\mathbf{R}^d	d-dimensional space
\mathcal{D}	Kullback-Leibler distance	$S_{u,mean}$	Average undrained shear strength (kPa)
E	Expectation	S_u	Undrained shear strength (kPa)
$E_p I_p$	Flexural rigidity of pile (kNm ²)	T	Iteration
E_{py}	Soil stiffness (kN/m ²)	\mathbf{t}	Vector of design variables
F	Failure domain	t	Iteration (counter)
H	Lateral load (kN)	t^*	Design point
g	Limit state	U	Uniform distribution
h	Distribution (Probability density function)	\mathbf{u}	Parametric vector
I	Indicator function	Var	Variance
K	Kernel pdf	\mathbf{v}	Parametric vector
k	Kernel sampling density estimator	V	Axial load (KN)
k	Number of nested sequence	W	Weight
L	Embedment depth (m)	w	Window width
N	Sample size	w	Wall thickness (m)
N_F	Number of failed samples	y	Pile lateral deflection along the pile (m)
M	Bending moment (kNm)	z	Position along the pile (m)

Greek Letters

α_p	Updating parameter for optimization (mean)
α_r	Updating parameter for reliability (mean)
β_p	Updating parameter for optimization (standard deviation)
β_r	Updating parameter for reliability (standard deviation)
β	Reliability index
$\boldsymbol{\theta}$	Random vector
λ	Local bandwidth factor

μ	Mean
σ	Standard deviation
γ	Intermediate probability of failure
γ'	Soil submerged unit weight (kN/m ³)
ρ	Correlation
ρ	Density (kg/m ³)
ρ	Percentage of failure at each iteration
ϕ	Correlation length (m)
Φ	Cumulative distribution function
ν	Poisson's ratio
ε_{50}	Strain at mean of S_u (m/m)

Abbreviations

CE	Cross-Entropy
C_oV	Coefficient of variation
COV	Covariance
FOSM	First Order Second Moment
IM	Importance Sampling
MC	Monte Carlo
MCMC	Markov Chain Monte Carlo
pdf	Probability distribution function
SA	Simulated Annealing
SS	Subset Simulation
SSO	Stochastic Subset Optimization
RBDO	Reliability-based design optimization

1. Introduction

1.1 Background

Engineering facilities such as bridges, power plants, dams and offshore platforms are intended to benefit the society at the expense of high construction cost. Unfortunately, the failure of these structures could result in public safety issues as well as economic and environmental consequences (Choi et al., 2006); therefore, the main concern of engineering design is to keep the structures safe (reliable) under the possible minimum (optimum) construction cost so that the probability of failure and cost of construction of the structures are reduced.

Different design approaches are currently in use based on the level of uncertainty in the input parameters (e.g. material properties, loads, etc.). For simple structures with relatively low uncertainties in the input parameters, a direct or deterministic approach using a factor of safety can be implemented (Choi et al., 2006). Another approach explained by Phoon (2008) is called Reliability-based design which is a probabilistic framework that considers uncertainties in the design parameters to produce a design with acceptably small failure probability.

Reliability-based design optimization (RBDO) is an advantageous methodology for design of engineering structures. The advantages of using RBDO are discussed by Valdebenito and Schuëller (2010) as it allows for determining the best design solution (reliable and optimum) while explicitly considering the unavoidable effects of uncertainties in engineering designs.

Various methods have been developed to solve reliability and optimization problems (Choi et al., 2006 and Schuëller et al., 2004). The main shortcoming of existing RBDO algorithms is that they are computationally demanding, because both reliability and optimization algorithms

can require large number of simulations of computationally complex models simulating the response of a structure or an engineering system.

This study implements an algorithm, known as Cross-entropy (CE), to solve both reliability and optimization problems within the RBDO. The performance of the Cross-entropy method is examined on an RBDO problem with an analytical solution and a practical problem of a monopile foundation for offshore wind turbine.

1.2 Objective of study

The main objective of this thesis is to demonstrate the advantages of the RBDO formulations in an engineering design and utilize the flexibility of the Cross-entropy method to deal with the reliability and optimization sub-problems within the RBDO problem. The objectives of this study are listed below:

- To identify and study existing reliability and optimization analysis methods.
- To evaluate the performance of the existing methods with respect to accuracy and efficiency.
- To identify and study methods for RBDO of structures.
- To prepare, develop and study the parameters of the CE algorithm.
- To validate the CE algorithm on an RBDO problem with an analytical solution.
- To compare the efficiency and accuracy of the CE algorithm with the existing reliability and optimization methods.
- Finally, to check and evaluate the CE algorithm by testing on a practical RBDO problem of a monopile foundation for offshore wind turbine.

1.3 Study Approach

Numerical modelling and simulations have been adopted for the implementation of the CE algorithm as well as to prepare algorithms for the existing reliability and optimization methods. A high level language, MATLAB (version R2014a and R2013b) developed by MathWorks company, has been utilized for the numerical modelling and simulations. The CE algorithm was prepared for reliability analysis and further developed to apply for optimization problems. Then, the developed CE algorithm is investigated and evaluated on an academic problem that has an analytical solution and finally implemented on a design of a monopile foundation for offshore wind turbine.

1.4 Scope of the Thesis

An algorithm that is used for RBDO is developed and tested on a monopile foundation for offshore wind turbine. The CE method is initially validated on an academic RBDO problem that has an analytical solution and the necessary parameter study for the CE algorithm is conducted. In the meantime, the efficiency and accuracy of the CE method have been evaluated by comparing it with existing reliability and optimization methods. Finally, the CE algorithm was tested and evaluated on a design of a laterally loaded monopile foundation for offshore wind turbine.

1.5 Limitation

The following are some of the limitations faced during this study:

- The evaluation of the CE method algorithm on an academic problem showed limitations for both reliability and optimization for large numbers of uncertain input parameters.
- Special attention should be given to parameter selection of the CE algorithm. Appropriate selection of the parameters can affect the final output.

1.6 Structure of the Thesis

The next chapters of the thesis are structured as follows:

Chapter 2 reviews some of the commonly used methods for reliability analysis and optimization in engineering. Moreover, several methods were implemented for comparison in terms of efficiency and accuracy.

Chapter 3 presents the Cross-entropy method with the general principles and discusses how the method is developed.

In Chapter 4, the implementation of the CE algorithm is described and the effect of parameter selection on the performance of the algorithm is investigated. The algorithm is tested on a problem with an analytical solution.

In Chapter 5, the CE algorithm is evaluated on a RBDO problem of a monopile foundation of wind turbine. Moreover, the analysis, results and discussion of the numerical simulations are presented.

In Chapter 6, important findings and conclusions drawn from the study as well as recommendations and possible future works in this area of study will be discussed.

2. Literature Review

2.1 Introduction

As modern engineering analysis requires more critical and complex design, the need for accurate approaches to assess uncertainties in computer models, soil parameters, strength, loads, material properties, manufacturing processes, geometries and operational environments have increased significantly (Choi et al., 2006).

Although for simple structures and relatively low uncertainty in the input parameters, a direct or deterministic approach using a factor of safety is implemented, (Choi et al., 2006), it is recommended by Phoon (2008) to apply a RBDO to quantify uncertainties in the design parameters to produce a robust design.

There exist various methods used for a RBDO based on different theoretical formulations. The main challenge when implementing these methods is that they are computationally intensive and time consuming. This is due to the nature of reliability and optimization algorithms which require large number of simulations of engineering models.

In this study, the Cross-entropy method is implemented to solve both reliability and optimization problems with in the RBDO. The detail principles of the Cross-entropy method will be discussed in Chapter 3.

The Cross-entropy method, proposed by Rubinstein (1997), was successfully applied in several fields of study such as: DNA sequence alignment (Keith and Kroese, 2002), network reliability optimization (Kroese et al., 2007), vehicle routing optimization with stochastic demands (Chepuri and Homem-de-Mello, 2005), mixed integer nonlinear programming (Kothari and Kroese, 2009), queueing models of telecommunication systems (De Boer et al.,

2004), project management (Cohen et al., 2005), optimal policy search (Busoniu et al., 2010) and noisy optimization problems such as optimal buffer allocation (Alon et al., 2005) are some of the products of the Cross-entropy method.

This literature review concentrates on some of the important reliability and optimization methods used to solve engineering problems; therefore, this literature review is presented in two sections-Reliability analysis methods and Optimization methods.

2.2 Reliability and Reliability Analysis Methods

According to Choi et al. (2006), reliability is defined as the probability that a system will perform well its function over a specified period of time and under specified service conditions. The performance of a system is evaluated with a performance function which defines the state of a system as safe or unsafe. The state of a system is commonly defined as serviceability limit state if the minimum limit of safety is based on the allowable deflection, vibration or settlement of the structure while ultimate limit state defines the maximum state on the collapse of part or whole structure. If the limit state is exceeded or the structure cannot perform for its intended function, the structure is unreliable. Therefore, reliability is concerned with probability of limit state violations at any stage during a structure's life.

Schuëller et al. (2004) describes the reliability problem for performance function, $g(\boldsymbol{\theta})$, using a given random vector, $\boldsymbol{\theta}$, distributed with a probability density, $h(\boldsymbol{\theta})$, over a d-dimensional space, \mathbf{R}^d . The failure region or domain is defined as $g(\boldsymbol{\theta}) \leq 0$, denoted by F , while $g(\boldsymbol{\theta}) > 0$ indicates the safe domain. Hence, the probability of failure, P_f , is defined on Equations (2.1) and (2.2) as:

$$P_f = \int_{g(\boldsymbol{\theta}) \leq 0} h(\boldsymbol{\theta}) d(\boldsymbol{\theta}) = \int_{\mathbf{R}^d} \mathbf{I}(\boldsymbol{\theta}) h(\boldsymbol{\theta}) d(\boldsymbol{\theta}) \quad (2.1)$$

$$P_f = \mathbf{P}[g(\boldsymbol{\theta}) \leq 0] = \mathbf{E}[\mathbf{I}(\boldsymbol{\theta})] \quad (2.2)$$

Where,

-The limit state, $g(\boldsymbol{\theta})=0$, defines the margin of safety between the stabilizing (resistance) and destabilizing of structures.

- $\boldsymbol{\theta}$ is a random vector denoting d number of uncertain inputs, $[\theta_1, \theta_2, \theta_3, \dots, \theta_d] \in \boldsymbol{\theta} \subset \mathbf{R}^d$.

- $\mathbf{I}(\boldsymbol{\theta})$ denotes the indicator function of F which equals 1 if $[g(\boldsymbol{\theta}) \leq 0]$ and 0 if $[g(\boldsymbol{\theta}) > 0]$.

$-P[g(\boldsymbol{\theta}) \leq 0]$ indicates probability of violation of the limit state and is expressed in terms of the expectation (mean), \mathbf{E} , of the indicator, $I(\boldsymbol{\theta})$.

Figure 2.1 shows the limit state region, failure and safe domains for two random vectors, θ_1 and θ_2 distributed with a probability density, $h(\boldsymbol{\theta})$.

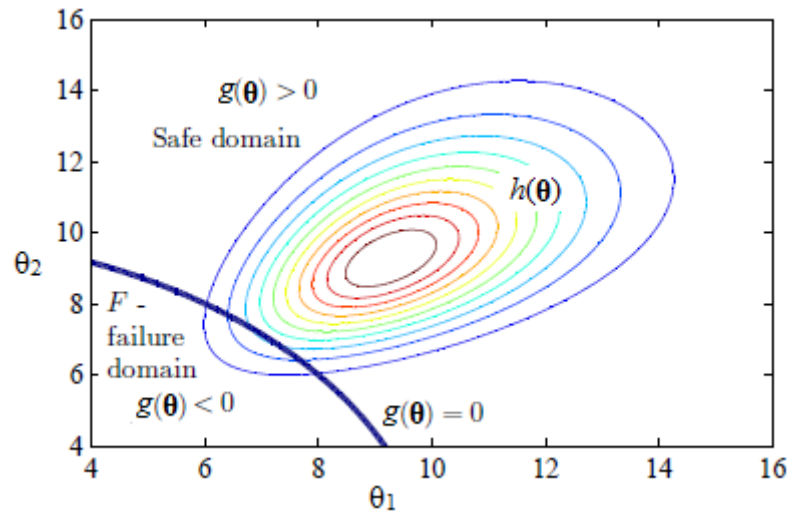


Figure 2.1 Reliability analysis between θ_1 and θ_2 on $h(\boldsymbol{\theta})$ (Adopted from (Depina, 2014)).

Various methods and approaches have been proposed by different scholars for calculation and estimation of the failure probabilities. These reliability analyses methods can be classified as Sampling (e.g. Monte Carlo, Importance Sampling and Subset Simulation) and Algorithms which apply optimization methods (e.g. FORM and SORM).

2.2.1 Sampling Methods

In the context of reliability analysis, sampling is related to the generation of random numbers which are values or outcomes associated with given random variables (Phoon, 2008). Random numbers can be generated by a True random number generator (generated by measuring a physical process that is expected to be random e.g. temperature fluctuation) or a Pseudo random number generic (generated by computer programming e.g. using MATLAB or Excel); therefore, these sets of all possible outcomes are called samples and are used to simulate the real cases in engineering problems to calculate the probability of failures and analysis of reliabilities.

The basic advantage of the sampling methods is explained by Choi et al. (2006) as their direct utilization of samples to obtain mathematical solutions or probabilistic information concerning problems whose system equations cannot be solved easily by known procedures.

The following section presents the general overview of the sampling methods together with their respective advantages and disadvantages. It is not intended to provide a complete and detail description with all the required mathematical analysis; instead, a general overview is presented. Monte Carlo simulation, Importance sampling and Subset simulation are categorized under sampling methods because the main inputs for the calculation of reliability or probability of failure is the set of random numbers generated (samples).

A. Monte Carlo Simulation (MC)

Monte Carlo simulation is described by Choi et al. (2006) as a powerful mathematical tool for determining the approximate probability of violation for a given limit state using random numbers and statistical analysis of trial outputs.

Algorithm of the Monte Carlo simulation can be summarized as follows:

1. Define the limit state, $g(\boldsymbol{\theta})$, of the system/structure as discussed in Section 2.2.
2. Identify the uncertain input parameters (e.g. shear strength, external load, etc.) associated within $g(\boldsymbol{\theta})$ and describe them probabilistically as random vector, $\boldsymbol{\theta}$, given by $[\theta_1, \theta_2, \theta_3, \dots, \theta_d] \in \boldsymbol{\theta}$ and $h(\boldsymbol{\theta})$.
3. Define the desired number of samples or number of simulations, N .
4. Generate a realization for each random variable with a sample size of N . Note here, d is the number of random variables while random numbers are generate with a sample size of N to simulate each random variable, for example, $\theta_1 = [\theta_1, \theta_2, \theta_3, \dots, \theta_N]$ and $\theta_2 = [\theta_1, \theta_2, \theta_3, \dots, \theta_N]$ for two-dimensional variable vectors, $d=2$.
5. Evaluate the response of the structure/system for a given combination of random parameters, $g(\boldsymbol{\theta})$.
6. Count the number of fails which give $g(\boldsymbol{\theta}) \leq 0$ and denote by N_F .
7. The probability of failure is then calculated as the ratio of N_F to N .

Similar to Equations (2.1) and (2.2) given for the failure probability estimation of the limit state, Equation (2.3a) gives the estimate of P_f for Monte Carlo method and the coefficient of variation, CoV , given by Equation (2.3b) is commonly used as a convergence parameter.

$$P_f = \frac{1}{N} \sum_{i=1}^N I(\theta_i) = \frac{N_F}{N} \quad (2.3a)$$

$$CoV(P_f) = \sqrt{\frac{1 - P_f}{N P_f}} \quad (2.3b)$$

Where, $I(\theta_i)$ equals 1 if $g(\theta_i) \leq 0$ and 0 if $g(\theta_i) > 0$, N_F is the number of failed samples (samples resulting $g(\theta_i) \leq 0$) and N is the total number of samples.

MC method is widely applied in reliability analysis of engineering structures because it provides robust estimates of failure probabilities. Moreover, it is not affected by the nonlinearity of the problem and is straightforward to implement. The performance of the method is also independent of the dimensionality of the problem.

The disadvantages of the Monte Carlo method can be stated as; MC requires large number of samples and model evaluations to simulate rare events¹ and it is inefficient in situations where complex models are used to simulate the response of the engineering structures because of computationally intensive simulations (e.g. finite element model).

B. Importance Sampling (IM)

Important sampling is developed from the Monte Carlo method by introducing a second distribution called importance distribution, $f(\boldsymbol{\theta})$, defined close to the failure region. The application of the importance distribution is intended to get efficient simulation of rare events in the reliability assessment of engineering structures so that the disadvantages of the Monte Carlo method can be overcome (Au et al., 1999).

According to Schuëller et al. (2004), the main principle of the IM method is to draw samples of random vector parameters, $\boldsymbol{\theta}$, from a distribution $f(\boldsymbol{\theta})$ which is concentrated in the ‘important region’ of the random parameter space that is the failure domain, F . Equation (2.4) gives the definition of P_f for a random vector, $\boldsymbol{\theta}$, with original distribution, $h(\boldsymbol{\theta})$, and importance distribution, $f(\boldsymbol{\theta})$. Basically, Equation (2.1) presented earlier is modified to give:

$$P_f = \int_{\mathbf{R}^d} \frac{I(\boldsymbol{\theta})h(\boldsymbol{\theta})}{f(\boldsymbol{\theta})} f(\boldsymbol{\theta}) d(\boldsymbol{\theta}) \quad (2.4)$$

As discussed above, the importance (optimal) distribution is defined on the failure region or close to the failure region. The variation between the true P_f and P_f obtained based on Equation (2.4) is defined by the variance of P_f . Schuëller et al. (2004) describes optimal importance distribution as the distribution which results in a variance equal or near to zero. The variance of P_f , $\text{Var}[P_f]$, is given by Equation (2.5) and for $\text{Var}[P_f] \approx 0$, the optimal importance distribution, $f_{opt}(\boldsymbol{\theta})$, is defined by Equation (2.6).

¹ Events that occur with relatively low occurrence of probability, $P_f < 10^{-4}$

$$\text{Var}[P_f] = \frac{1}{N} \left(\int_{\mathbf{R}^d} \frac{I(\boldsymbol{\theta})h^2(\boldsymbol{\theta})}{f^2(\boldsymbol{\theta})} f(\boldsymbol{\theta})d(\boldsymbol{\theta}) - P_f^2 \right) \quad (2.5)$$

$$f(\boldsymbol{\theta}) = f_{opt}(\boldsymbol{\theta}) = \frac{I(\boldsymbol{\theta})h(\boldsymbol{\theta})}{P_f} \quad (2.6)$$

Where,

$f(\boldsymbol{\theta})$ = Importance region probability distribution (pdf)

$I(\boldsymbol{\theta})$ = Indicator function of F

$h(\boldsymbol{\theta})$ = Original probability distribution (pdf)

N = Number of samples

The representation of Equation (2.6) is practically infeasible since it requires knowledge of P_f as a priori. Therefore, several techniques have been developed to approximate the optimal importance distribution and the most prevalent two approaches are the use of design point and kernel density approximation of the samples in the failure domain (Schueller et al., 2004). These two approaches are discussed below.

Schueller and Stix (1987) and Freudenthal (1956) initially propose the use of a design point, which may be defined as the closest point on the limit state function to the origin of the standard normal space (center of the $h(\boldsymbol{\theta})$), to be used as the center for the importance distribution. But Schueller et al. (2004) modifies the assumption and suggested the design point to be used if true additional information on the limit state is not possible to get. This is because the design point and their neighborhood do not always represent the most ‘important’ region of the failure domain, especially in high dimensional spaces. Furthermore, the computational cost associated to determine the design point can be quite high for complex limit state functions which adversely affect the efficiency of the method.

Figure 2.2 shows the importance distribution illustration. The design point is given as the closest point on the limit state at failure, $g(\boldsymbol{\theta})=0$, to the center of $\boldsymbol{\theta}=[\theta_1, \theta_2]$ with $h(\boldsymbol{\theta})$.

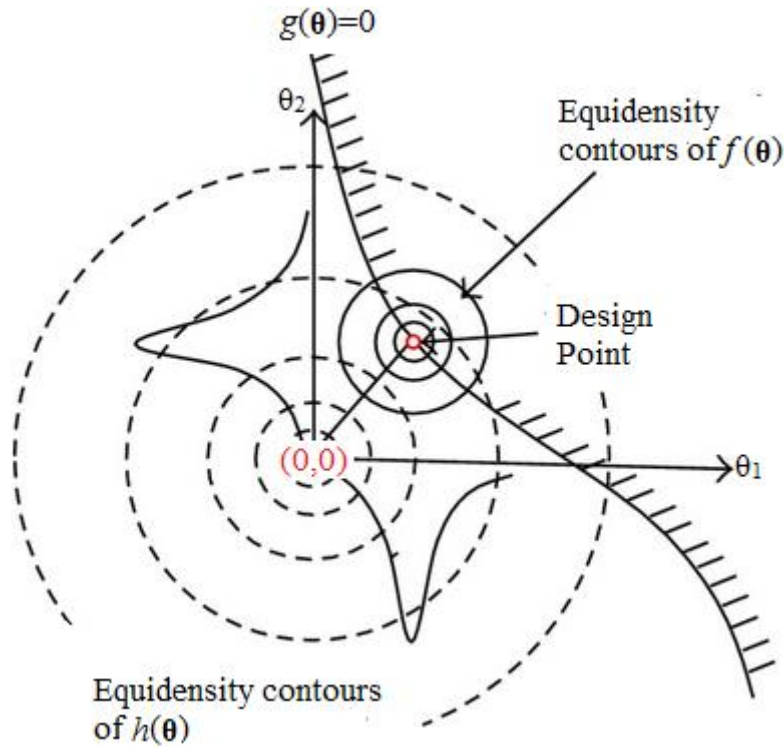


Figure 2.2 Importance distribution illustration (Adopted from (Gu, 2014))

To overcome the limitation posed on the use of the design point as the center of importance distribution and get more efficient estimate of P_f , points lying inside the failure domain, F , are used to construct a kernel sampling density estimator of the optimal importance sampling density (Schuëller et al., 2004). Kernel sampling density estimator, $k(\boldsymbol{\theta})$, is given by Equation (2.7).

$$k(\boldsymbol{\theta}) = f_{opr}(\boldsymbol{\theta}) = \frac{1}{N} \left(\sum_{i=1}^N \frac{1}{(w\lambda_i)^d} K \left(\frac{\boldsymbol{\theta}_0 - \boldsymbol{\theta}_i}{w\lambda_i} \right) \right) \quad (2.7)$$

Where,

$\boldsymbol{\theta}_0$ = initial point inside the failure domain, F

$\boldsymbol{\theta}_i$ = samples generated using advanced sampling methods such as Markov Chain and Markov Chain Monte Carlo (Gilk, 2005).

N = number of samples

w = window width

λ_i = local bandwidth factor

d = dimension

$K(\boldsymbol{\theta})$ = kernel pdf which is most commonly selected as the normal pdf (Schuëller et al., 2004 and Au et al., 1999). It is given by Equation (2.8) as:

$$K(\boldsymbol{\theta}) = \prod_{i=1}^d \left(\frac{1}{\sqrt{2\pi}} e^{-\frac{\theta_i^2}{2}} \right) \quad (2.8)$$

The quality of the estimate of the optimal sampling pdf, f_{opt} , provided by Equation (2.7) depends on the particular parameters θ_0 , w , λ_i and $K(\boldsymbol{\theta})$, and probabilistic characteristics of the points, θ_i , used. (Methods proposed by Au et al. (1999) and Schraudolph (1995) can be referred for detail estimation and selection of the parameters θ_0 , w and λ_i).

Finally, $k(\boldsymbol{\theta})=f_{opt}(\boldsymbol{\theta})$ is used as the importance sampling density in order to estimate P_f when substituted in Equation (2.6).

As a conclusion, the IM method can result in a reduced computational time and increased accuracy in estimation of small failure probabilities as compared to the Monte Carlo method (Schuëller et al., 2004 and Au et al., 1999).

C. Subset Simulation (SS)

Au et al. (1999) introduced the Subset simulation method for estimation of rare events failure probabilities of structural reliability problems. As the name subset indicates, the method uses a sequence of nested “failure” regions to reach the final failure region. The general concept and implementation technique is discussed below.

Au et al. (2001) consider the failure domain, F , defined by the condition $g(\boldsymbol{\theta}) \leq 0$, in which g is the performance function and $\boldsymbol{\theta}$ is a vector of random variables. Intermediate “failure” domain, F_i , is then defined by the condition $g(\boldsymbol{\theta}) < C_i$, in which C_i is a positive number. Further assumption is done that, it is possible to construct a nested sequence of failure domains of decreasing size using an increasing sequence of positive numbers, that is, there exists $C_1 > C_2 > \dots > C_k = 0$ such that $F_1 \supset F_2 \supset \dots \supset F_k$ and $P(F_k) = \prod_{i=1}^k P(F_i)$, where k denotes the number of nested sequence of failure domains. As C_i approaches to zero, F_i approaches to F given by the region $g(\boldsymbol{\theta}) \leq 0$.

Equations (2.9a) and (2.9b) define the failure probability, P_f , based on the nested sequence of failure domains or subsets as a product of a sequence of conditional probabilities.

$$P_f = P(F_1) \prod_{i=1}^{k-1} P(F_{i+1} | F_i) \quad (2.9a)$$

$$= P(F_k | F_{k-1})P(F_{k-1} | F_{k-2}) \dots P(F_2 | F_1)P(F_1) \quad (2.9b)$$

Therefore, P_f is a function of both the initial “failure”, $P(F_1)$, and the conditional probabilities $\{P(F_{i+1} | F_i) : i = 1, 2, \dots, k-1\}$. Then, $P(F_1)$ is calculated using the Monte Carlo simulation as discussed in Section 2.2.1(A). For the evaluation of the conditional probabilities, samples of θ given that they lie in the intermediate failure regions, F_i , are necessary. These samples are generated from $h(\theta|F_i)$ and are different from the samples generated from the original distribution, $h(\theta)$. Therefore, sampling of these points from the conditional distribution is done using Monte Carlo Markov Chain (MCMC) method (Gilk, 2005).

Equation (2.10) defines the conditional probability in terms of the indicator function, $I(\theta_j)$ for samples, θ_j , $j=1, 2, 3, \dots, N$, where sample size, N and number of nested sequence of failure domains, k , given by $i=1, 2, \dots, k-1$.

$$P(F_i | F_{i-1}) = \frac{1}{N} \sum_{j=1}^N I(\theta_j) \quad (2.10)$$

Au et al. (2001) describes the main advantage of the Subset simulation to be the ability to result in a faster convergence rate which does not depend on the number of random variables appearing in the problem. This is explained by Phoon (2008) and Schuëller et al. (2004) using a coefficient of variation, CoV , for the conditional probabilities, $P(F_i|F_{i-1})$. The relation can be seen in Equation (2.11) for N number of independent samples.

$$CoV_{(P(F_i|F_{i-1}))} = \sqrt{\frac{1 - P(F_i | F_{i-1})}{N * P(F_i | F_{i-1})}} \quad (2.11)$$

Moreover, the SS method is expected to reduce computational efforts in estimating small failure probabilities when compared to the Monte Carlo method because the estimation of the conditional probabilities can be performed accurately with a relatively small numbers of samples.

2.3 Reliability Methods which apply optimization methods

The reliability methods: FOSM (First-Order Second Moment), FORM (First-Order Reliability Method) and SORM (Second-Order Reliability Method) are based on calculation of the reliability index for estimation of P_f . Reliability index is defined as the shortest distance between the origin of the standard normal space (center of original distribution, $h(\boldsymbol{\theta})$) and the design point located on $g(\boldsymbol{\theta})$. FORM and SORM methods are classified as reliability methods which apply optimization in search for the design points.

A. First-Order Second-Moment (FOSM) Method

FOSM is a relatively simple reliability method which uses first-order Taylor's series expansion of $g(\boldsymbol{\theta})$ at the mean together with the first two moments (mean and variance) of the random variables, $\boldsymbol{\theta}$, to calculate the second moment (mean and variance) of $g(\boldsymbol{\theta})$ (Elishakoff et al., 1987).

The first two moments of the d number of random vectors; $\theta_1, \theta_2, \theta_3, \dots, \theta_d$ are given by Equation (2.12):

$$\mu = \{\mu_{\theta_1}, \mu_{\theta_2}, \dots, \mu_{\theta_d}\} \text{ and } \sigma = \{\sigma_{\theta_1}, \sigma_{\theta_2}, \dots, \sigma_{\theta_d}\} \quad (2.12)$$

The mean and variance (second moments) of $g(\boldsymbol{\theta})$ are also defined in Equations (2.13a) and (2.13b). Equation (2.13c) gives the variance of $g(\boldsymbol{\theta})$ for uncorrelated (independent) random vectors:

$$\mu_g = \mathbf{E}(g) \approx g(\mu_{\theta_1}, \mu_{\theta_2}, \dots, \mu_{\theta_d}) \quad (2.13a)$$

$$\text{Var}[g] = \sigma_g^2 \approx \sum_{i=0}^d \sum_{j=1}^d \text{COV}(\theta_i, \theta_j) \left(\frac{dg}{d\theta_i}, \frac{dg}{d\theta_j} \Big|_{\mu} \right) \quad (2.13b)$$

$$\text{Var}[g] = \sigma_g^2 \approx \sum_{i=1}^m \left(\sigma_{\theta_i} \frac{dg}{d\theta_i} \Big|_{\mu} \right)^2 \quad (2.13c)$$

Where,

μ_g = Mean of the performance function, $g(\boldsymbol{\theta})$

σ_g = Standard deviation of the performance function, $g(\boldsymbol{\theta})$

$\mathbf{E}(g)$ = Expectation (mean) of performance function, $g(\boldsymbol{\theta})$

$\text{COV}(\theta_i, \theta_j) = \mathbf{E}[(\theta_i - \mu_{\theta_i})(\theta_j - \mu_{\theta_j})] = \text{Covariance between } \theta_i \text{ and } \theta_j$

Therefore, the reliability index, defined as the shortest distance between the origin and the design point, is calculated as: $\beta = \frac{\mu_g}{\sigma_g}$ and the failure probability, P_f , is commonly calculated under the assumption that g is normally distributed: $P_f = 1 - \varphi(\beta) = \varphi(-\beta)$, where φ is the probability distribution function.

Elishakoff et al. (1987) and Choi et al. (2006) listed the disadvantages of the FOSM method such as: lower accuracy for second and higher order performance functions (uses only first-order Taylor's series), full distribution is not used (only the mean and standard deviation are incorporated), the skewness and higher moments are ignored (commonly normal distribution is assumed) and reliability index is not uniquely defined (depends on the formulation of $g(\boldsymbol{\theta})$).

B. First-Order Reliability Method (FORM)

FORM is an analytical approximation in which the reliability index is interpreted as the minimum distance from the origin of the standard space to the limit state surface (Fiessler et al., 1979). It is based on the first order Taylor's series expansion at the design point, rather than the mean in case of the FOSM.

As discussed in Section 2.2.1(B), the location of the design point is difficult to obtain for non-linear or higher order performance functions. Hasofer-Lind (H-L) Algorithm which is explained in detail by Hasofer and Lind (1974) is commonly used to get a good estimate on the location of the design point (Refer: (Hasofer and Lind, 1974) for detail); therefore, the reliability index, β , can be obtained as the distance between the origin and the design point. Similar to the FOSM method, the probability of failure can be obtained from the reliability index, $P_f = 1 - \varphi(\beta) = \varphi(-\beta)$.

The merit of FORM method over the FOSM is stated by Fiessler et al. (1979) and Choi et al. (2006) such as: reliability index is uniquely defined (not dependent on the formulation of $g(\boldsymbol{\theta})$) and the method incorporates full distributions (distribution based on design point, $f(\boldsymbol{\theta})$). But the accuracy of the method is low in case where the performance function is non-linear (second and higher orders performance functions). Moreover, in case of multiple design points and random variables, the algorithm needs several runs with independent starting points (Tichý, 1994) and (Fiessler et al., 1979).

C. Second-Order Reliability Method (SORM)

SORM utilizes second order approximation at the design point to define $g(\boldsymbol{\theta})$. SORM is more accurate than the FORM method for a non-linear definition of $g(\boldsymbol{\theta})$, but it can be computationally more expensive (time consuming) and difficult since it requires the second order derivatives of $g(\boldsymbol{\theta})$ at the design point (Fiessler et al., 1979).

The approximation of a non-linear $g(\boldsymbol{\theta})$ using both the FORM and SORM is given by Figure 2.3 and it can be observed for non-linear $g(\boldsymbol{\theta})$, SORM provides a better approximation than the FORM at the design point. Tichý (1994) explains that the efficiency of both methods decrease as the non-linearity of $g(\boldsymbol{\theta})$ increase and the knowledge on the location of the design point is important for a good estimate of P_f .

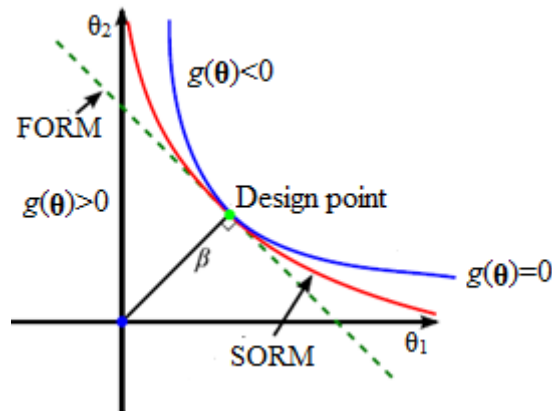


Figure 2.3 Approximation of non-linear $g(\boldsymbol{\theta})$ using FORM and SORM (Depina, 2014)

2.3.1 Justification of Reliability Methods using a Non-linear Example

In the previous sections, an overview and principles of some of the reliability methods used in engineering design have been discussed. The aim of this section is to compare the performance of several reliability methods on a simple problem. Therefore, a simple non-linear performance function, $g(\boldsymbol{\theta})$, with random variables, θ_1 and θ_2 , is considered as given by Equation (2.14).

$$g(\boldsymbol{\theta}) = 0.5^{\theta_1} - \theta_2 + 2.5 \quad (2.14)$$

The calculation of P_f for the given performance function on Equation (2.14) is assessed using FOSM, FORM, MC, IM and SS methods. The calculations and preparation of the algorithms for these methods are based on the literature review discussed in Section 2.2.

For this particular example, a normal distribution ($\mu=0$ and $\sigma=1$) is assumed for the variable vectors of random numbers (θ_1 and θ_2). Different sample sizes, N , are selected to investigate

the effects on the accuracy of the final result. Figure 2.4 shows the sample distribution generated using sample size of $N=1000$.

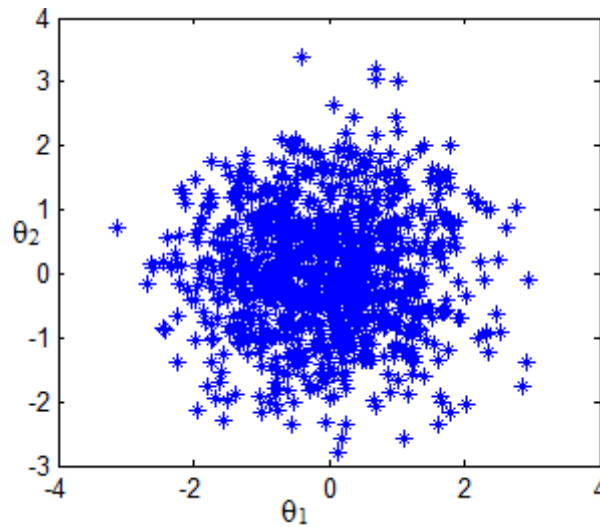


Figure 2.4 Distribution of variable vectors for $N=1000$ (normal distributions)

Assessment based on FOSM approximation gave, $\mu_g=3.5$ and $\sigma_g=1.217$. Therefore, $\beta = 2.877$, and the respective probability of failure, $P_f=2 \times 10^{-3}$. For the FORM approximation the design point and reliability index, β , were obtained using Hasofer Lind (H-L) Algorithm. The design point was obtained to be (1.111, 2.956) and the reliability index, β converged to 3.1584 after four iterations; therefore, $P_f=7.9 \times 10^{-4}$.

In case of IM, a second normal distribution at the design point, $f_{opt}(\theta)$, with $\mu=(1.111, 2.956)$ and $\sigma = 1$, was introduced. The Subset simulation is also implemented to compute small probability of failures. The sample sizes for the Subset simulation are given here per step of the nested series as the method is defined in a sequence of failure regions. The number of steps was observed to be four in this particular problem. Table 2-1 below shows the complete summary of the probability of failures results for different sample size, N .

Table 2-1 Estimated P_f values using FOSM, FORM, MC, IM and Subset simulation for different sample sizes, N

Sample size, N	100	500	1,000	10,000	100,000	1,000,000
FOSM, P_f	2.00e-03					
FORM, P_f	7.90e-04					
MC, P_f	0	0.004	1.00e-03	9.00e-04	5.70e-04	5.96e-04
IM(Importance sampling), P_f	6.40e-04	6.44e-04	5.93e-04	6.09e-04	6.02e-04	6.00e-04
Subset simulation, P_f	5.00e-04	4.08e-04	3.85e-04	7.10e-04	7.95e-04	7.52e-04

It can be seen from Table 2-1, for the non-linear performance function, the application of the FOSM approximation method resulted in a higher failure probability estimate. FORM and FOSM are based on first order approximation but the FORM gave a good estimate of P_f similar to the Importance sampling and Subset simulation method because the design point location was calculated without difficulty using the Hasofer Lind (H-L) algorithm as a priori.

As discussed in Section 2.2.1(A), the Monte Carlo simulation required large number of samples ($N > 10,000$) to obtain an estimate of P_f with accuracy similar to the Importance sampling and Subset simulation methods. The accuracy of the MC improved with increase in the sample size but resulted in an intensive computation.

Both the Importance sampling and Subset simulation required smaller sample sizes to give rare events $P_f (< 10^{-4})$. Here, it can be noted that, the IM is performing well because the design point location was accurately known using the Hasofer Lind (H-L) Algorithm and this design point is used for an approximation of the optimum distribution, $f_{opt}(\theta)$.

Although for the Subset simulation, $N=100$ gives a good estimate of P_f as discussed above, Figure 2.5 illustrates the Subset simulation procedure with a sample size, $N=10,000$. Similar to discussion on Section 2.2.1(C), the P_f is obtained as a product of series of conditional failure probabilities (levels) as shown in Figure 2.5.

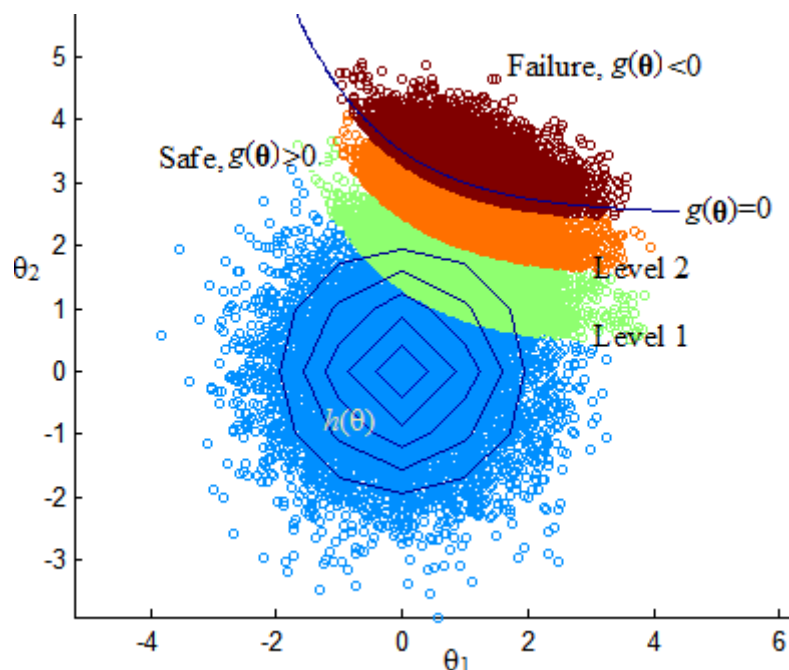


Figure 2.5 Subset simulation result for $N=10,000$ samples

Generally, the analysis results and observations based on the simple non-linear performance function example agree well with the details in the literature review of Section 2.2.

2.4 Reliability-Base design Optimization (RBDO)

Optimization is the act of obtaining the best result from given circumstances such as construction cost, reliability, performance and maintenance to meet an optimal structure (Choi et al., 2006). RBDO is concerned with the minimizations of expected life time costs considering construction and maintenance costs together with eventual failure (Kupfer and Freudenthal, 1977).

RBDO allows for determining the best design solution in terms of reliability and cost while explicitly considering the unavoidable effects of the uncertain input parameters (Valdebenito and Schuëller, 2010).

In the previous sections different reliability analysis methods have been discussed while this section will provide an insight into the commonly used optimization methods.

Problem definition

The general RBDO problem is presented by Equation (2.15) as given by Kupfer and Freudenthal (1977) and Royset et al. (2001).

Minimize: The objective function, $C(\boldsymbol{\theta}, \mathbf{t})$ (2.15a)

Subjected to

$$g_j(\boldsymbol{\theta}, \mathbf{t}) \leq 0, \quad j = 1, \dots, n_t, \text{ inequality constraints} \quad (2.15b)$$

$$h_k(\boldsymbol{\theta}, \mathbf{t}) = 0, \quad k = 1, \dots, s, \text{ equality constraints} \quad (2.15c)$$

$$(\boldsymbol{\theta}^l, \mathbf{t}^l) \leq (\boldsymbol{\theta}, \mathbf{t}) \leq (\boldsymbol{\theta}^u, \mathbf{t}^u), \text{ upper and lower bounds} \quad (2.15d)$$

Where,

$$\boldsymbol{\theta} = [\theta_1, \theta_2, \dots, \theta_d] \in \Omega_{\boldsymbol{\theta}} \subset \mathbf{R}^d, \quad \Omega_{\boldsymbol{\theta}} \text{ is the space of random parameters.}$$

$$\mathbf{t} = \text{Design variables} = [t_1, t_2, \dots, t_n] \in \Omega_{\mathbf{t}} \subset \mathbf{R}^n, \quad \Omega_{\mathbf{t}} \text{ is the space of design variables.}$$

A design variable is defined by Royset et al. (2001) as a numerical input that is allowed to change during the design optimization in order to satisfy the objective function, e.g. until the minimum or optimum cost is obtained.

The inequality constraints, given by Equation (2.15b) are commonly applied within a RBDO to compare P_f of the structure with the allowable (tolerable) failure, $P_f < P_f^{\text{tol}}$.

Various approaches and methods have been implemented to solve RBDO problems. Some of the most common optimization methods applied in engineering includes: Double-loop

approach, Decouple approach and Stochastic Subset optimization (SSO) approach (Valdebenito and Schuëller, 2010)

A. Double-Loop Approach

Double-Loop approach is the most direct approach to solve RBDO problems which considers only the inequality constraint (Enevoldsen and Sørensen, 1994). As the name double-loop implies, each set of the design variables, \mathbf{t} , are initially used to estimate the objective function, $C(\mathbf{t})$ and later evaluated based on the inequality constraint of the reliability index, $\beta(\mathbf{t}) \geq \beta^{tol}$. The reliability problem can be solved using one of the methods discussed in Section 2.3 while the objective function, $C(\mathbf{t})$, is solved using an optimization algorithm such as a powerful method called simulated annealing (this method will be presented at the end of this section).

As can be seen in Equation (2.16) below, each set of design variable is first evaluated using $C(\mathbf{t})$ and again the design variables are used to check the reliability index, $(\beta(\mathbf{t}) \geq \beta^{tol})$. The problem definition of this method is given by Equation (2.16).

Minimize: The objective function, $C(\mathbf{t})$ (2.16a)

Subjected to

$$\beta(\mathbf{t}) \geq \beta^{tol} \quad (2.16b)$$

Where, $\beta(\mathbf{t})$ is the reliability index associated with the probability of failure of the structure and β^{tol} is the minimum acceptable reliability index, which is defined as: $\beta^{tol} = \Phi^{-1}(1 - P_f^{tol})$

Dubourg et al. (2010) argue that despite the conceptual simplicity of the double-loop approach, it lacks efficiency since it requires too many evaluations of the performance functions for each set of design variables, \mathbf{t} , which might result in a time consuming computation. However, for a broad range of applications where the performance functions are linear or weakly non-linear, it can give results within a reasonable number of evaluations of the performance functions.

Simulated Annealing (SA)

One of the robust optimization tools used to solve high dimensional design problems is the *Simulated Annealing (SA)*. Annealing is a thermal process for obtaining low energy states (by reducing temperature) of a solid in a heat bath; therefore, annealing process contains two steps which involve increasing the temperature until the solid molecules melt (change to gas state) and decreasing carefully the temperature (gentle cooling) until particles arrange themselves to

give the minimum energy state of the solid (Goffe et al., 1994). This process of annealing can be seen in Figure 2.6.

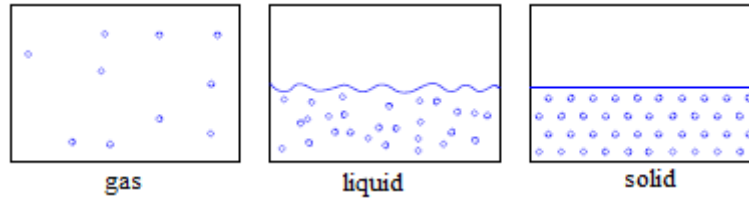


Figure 2.6 Cooling process of particles to yield low energy state (Depina, 2014)

Aarst and Korst (1989) explain the analogy with an optimization problem. The optimum cost is assumed to be equivalent to the energy state and the solutions in the optimization problem are equivalent to the resulting temperature in the final state of the physical system (global minima).

The advantages of using the Simulated annealing to solve optimization problems are discussed by Goffe et al. (1994). Not only can Simulated annealing find the global optimum (minimum), it is also less likely to fail on complex and discontinuous functions because it is a very robust algorithm.

B. Decouple Approach

Tu et al. (2001) proposed a method called *decouple approach* that avoids a double-loop problem associated with the RBDO. In this approach, for randomly generated design variables, t_i , of sample size, N , a linear approximation of the reliability index is constructed using derivatives of the failure probability as shown in Equation (2.17) Then the appropriate design variables which yield $\beta(\mathbf{t}) \geq \beta^{tol}$ are extracted and used to solve the optimization problem, $C(\mathbf{t})$. By doing this, double-looping and double checking of the set of design variables is ignored and can improve numerical efficiency.

Equation (2.17) shows the key step in this approach which is the construction of a linear approximation of the reliability index using information on the gradients of the failure probability, i.e.:

$$\beta(\mathbf{t}) = \beta(\mathbf{t}^b) + \sum_{i=1}^N \left. \frac{\partial \beta(\mathbf{t})}{\partial t_i} \right|_{t=\mathbf{t}^b} (t_i - t_i^b) \quad (2.17)$$

Where,

\mathbf{t} = design variable of randomly generated numbers, $[t_1, t_2, \dots, t_N]$, with sample size, N .

\mathbf{t}^b = the b-th candidate optimal design which yields $\beta(t_i) \geq \beta^{tol}$

b = order of candidacy which define 't_i' which yield $\beta(t_i) \gg \beta^{tol}$ is better candidate than 't_i', $\beta(t_i) \geq \beta^{tol}$.

Since the decoupling approach requires the calculation of derivatives, it might result in time consuming computations for complex objective functions (Royset et al., 2001 and Du and Chen, 2004).

C. Stochastic subset optimization (SSO)

Stochastic subset optimization is a simulation based approach recently proposed by Taflanidis and Beck (2008) that concentrates to find the region of admissible design space (region where the failure probability density function is minimum).

The overall concept is closely related with the Subset simulation reliability analysis method, discussed in Section 2.2.1(C). However, the major drawback of the method is that the problem that SSO attempts to solve is not a full RBDO problem in the sense that it is designed to minimize the failure probability whereas the purpose of the RBDO is to minimize a cost function under some failure probability constraint as given by Equation (2.15b) and (2.16b).

3. Cross-Entropy Algorithm for Reliability analysis and Optimization

3.1 Introduction

The core of this study is to prepare and implement the Cross-entropy (CE) algorithm to solve RBDO problems. The Cross-entropy method was proposed by Rubinstein (1997) based on the basic principle of Importance sampling procedures to estimate failure probabilities of rare-events ($<10^{-4}$). Subsequent work by Rubinstein (1999; 2001) has also shown a small modification of Rubinstein (1997) can be used to solve optimization problems so that the optimization problems are translated in to rare-event estimation problems.

The discussion on Chapter 2 Section 2.2.1(B) about Importance sampling method explained how the optimal distribution, $f_{opt}(\boldsymbol{\theta})$, on the failure region can be obtained from the initial distribution, $h(\boldsymbol{\theta})$, based on variance minimization. It was also pointed out that $f_{opt}(\boldsymbol{\theta})$ is approximated commonly based on design points. The computational cost associated to determine the design point can be quite high for complex limit state functions which adversely affect the efficiency of the Importance sampling method.

This chapter will introduce the CE method with the basic principles. The development of the algorithm for both reliability and optimization analysis are also presented. Moreover, it discusses how the optimal distribution, $f_{opt}(\boldsymbol{\theta})$, can be obtained relatively easier by implementing the CE method.

3.2 Cross-Entropy for Rare-event Probability Estimation

As discussed previously in Section 2.2, the probability of failure is given by Equations (2.1) and (2.2) as:

$$P_f = \int_{g(\boldsymbol{\theta}) \leq 0} h(\boldsymbol{\theta}) d(\boldsymbol{\theta}) = \int_{\mathbf{R}^d} \mathbf{I}(\boldsymbol{\theta}) h(\boldsymbol{\theta}; \mathbf{u}) d(\boldsymbol{\theta}) \quad (3.1)$$

$$P_f = \mathbf{P}[g(\boldsymbol{\theta}) < 0] = \mathbf{E}[\mathbf{I}(\boldsymbol{\theta})] \quad (3.2)$$

Where,

$\boldsymbol{\theta} = [\theta_1, \theta_2, \theta_3, \dots, \theta_d]$, random vector, is distributed with a pdf, $h(\cdot; \mathbf{u})$

\mathbf{u} = parametric vector (e.g., mean and standard deviation) of random vector, $\boldsymbol{\theta}$, in a given space, \mathbf{R}^d

\mathbf{E} = expectation is also defined in terms of the indicator function, $\mathbf{I}(\boldsymbol{\theta})$

$g(\boldsymbol{\theta})$ = limit state function

The discussion in Section 2.2.1(B) and Equation (2.4) gave the Importance sampling method for estimation of the probability of failure which is the base for the CE method. The P_f is given by Equation (3.3) as:

$$P_f = \int_{\mathbf{R}^d} \frac{\mathbf{I}(\boldsymbol{\theta}) h(\boldsymbol{\theta})}{f(\boldsymbol{\theta})} f(\boldsymbol{\theta}) d(\boldsymbol{\theta}) = \frac{1}{N} \sum_{i=1}^N \mathbf{I}(\theta_i) \frac{h(\theta_i)}{f(\theta_i)} \quad (3.3)$$

Where, $f(\boldsymbol{\theta})$ = Importance distribution (pdf) and $[\theta_1, \theta_2, \theta_3, \dots, \theta_N]$ are randomly generated numbers using sample size of N for simulation of a given random variable.

Schuëller et al. (2004) describes optimal importance distribution as the distribution which results in a variance of P_f equal to zero (or near to zero). Equations (2.5) and (2.6) presented the optimal importance distribution, $f_{opt}(\boldsymbol{\theta})$, as given by Equation (3.4).

$$f(\boldsymbol{\theta}) = f_{opt}(\boldsymbol{\theta}) = \frac{\mathbf{I}(\boldsymbol{\theta}) h(\boldsymbol{\theta})}{P_f} \quad (3.4)$$

A major drawback in the implementation of the optimal distribution is the definition based on an unknown P_f . The advantage of the CE method is that it provides a simple adaptive procedure for estimating the near optimal distribution using the concept of Kullback-Leibler divergence method in which the basic concept is discussed next.

3.2.1 Kullback-Leibler distance

It is described above that for a given initial distribution, $h(\boldsymbol{\theta}; \mathbf{u})$, the main aim of the IM method is to attain the $f_{opt}(\boldsymbol{\theta})$. Therefore, the idea of CE method is to choose the importance sampling distribution, $f_{opt}(\boldsymbol{\theta})$, from within the parametric class of pdfs, $h(\cdot; \mathbf{v})$. The parameter vector, \mathbf{v} , is selected such that the Kullback-Leibler distance between the optimal importance sampling pdf, $f_{opt}(\boldsymbol{\theta})$, and $h(\cdot; \mathbf{v})$ is minimal (De Boer et al., 2005 and Botev et al., 2013). The parametric vector is defined as a vector of distribution parameters (e.g., mean and standard deviation).

For a given independent random vectors $[\theta_1, \dots, \theta_d]$ with pdf of $h(\boldsymbol{\theta})$, the Kullback-Leibler distance between $f_{opt}(\boldsymbol{\theta})$ and $h(\cdot; \mathbf{v})$ is given by Equation (3.5) as defined by De Boer et al. (2005) and Botev et al. (2013).

$$\mathcal{D}(f_{opt}, h) = \int f_{opt}(\boldsymbol{\theta}) \ln \frac{f_{opt}(\boldsymbol{\theta})}{h(\boldsymbol{\theta})} d\boldsymbol{\theta} = \mathbf{E} \left[\ln \frac{f_{opt}(\boldsymbol{\theta})}{h(\boldsymbol{\theta})} \right], \quad \boldsymbol{\theta} \sim f_{opt}(\boldsymbol{\theta}) \quad (3.5a)$$

$$= \int f_{opt}(\boldsymbol{\theta}) \ln f_{opt}(\boldsymbol{\theta}) d\boldsymbol{\theta} - \int f_{opt}(\boldsymbol{\theta}) \ln h(\boldsymbol{\theta}; \mathbf{v}) d\boldsymbol{\theta} \quad (3.5b)$$

\mathcal{D} is not a distance in formal sense because $\mathcal{D}(f_{opt}, h) \neq \mathcal{D}(h, f_{opt})$.

Where,

\mathbf{u} = parametric vector (e.g., vector of mean and standard deviation) at initial distribution.

\mathbf{v} = parametric vector (e.g., vector of mean and standard deviation) between $h(\cdot; \mathbf{u})$ and $f_{opt}(\boldsymbol{\theta})$.

Minimizing the Kullback-Leibler distance given in Equations (3.5a) and (3.5b) is equivalent to choosing \mathbf{v} such that $-\int f_{opt}(\boldsymbol{\theta}) \ln h(\boldsymbol{\theta}; \mathbf{v}) d\boldsymbol{\theta}$ is minimized, which is the same as the maximization problem given by Equation (3.6).

$$\max_{\mathbf{v}} \int f_{opt}(\boldsymbol{\theta}) \ln h(\boldsymbol{\theta}; \mathbf{v}) d\boldsymbol{\theta} \quad (3.6)$$

Substituting $f_{opt}(\boldsymbol{\theta})$ from Equation (3.4) in to (3.6), the maximization is given by Equation (3.7) as:

$$\max_{\mathbf{v}} \int \frac{I(\boldsymbol{\theta}) \ln h(\boldsymbol{\theta}; \mathbf{v})}{P_f} h(\boldsymbol{\theta}; \mathbf{v}) d\boldsymbol{\theta} \quad (3.7a)$$

$$\max_{\mathbf{v}} \mathcal{D}(\mathbf{v}) = \max_{\mathbf{v}} E_h I(\boldsymbol{\theta}) \ln h(\boldsymbol{\theta}; \mathbf{v}) \quad (3.7b)$$

Where \mathcal{D} is implicitly defined above. Using the IM method, Equation (3.7) can be rewritten with a change of measure $h(\cdot; w)$ as given by Equation (3.8):

$$\max_{\mathbf{v}} \mathcal{D}(\mathbf{v}) = \max_{\mathbf{v}} E_w \mathbf{I}(\boldsymbol{\theta}) W(\boldsymbol{\theta}; \mathbf{u}; w) \ln h(\boldsymbol{\theta}; \mathbf{v}) \quad (3.8)$$

Where, W is the weight of the distribution given for any reference parameter w , with respect to the initial distribution, $h(\cdot; \mathbf{u})$:

$$W(\boldsymbol{\theta}; \mathbf{u}; w) = \frac{h(\boldsymbol{\theta}; \mathbf{u})}{h(\boldsymbol{\theta}; w)} \quad (3.9)$$

The optimal solution (\mathbf{v}^*) of Equation (3.8) can be written as shown in Equation (3.10) given by De Boer et al. (2005) and Botev et al. (2013).

$$\mathbf{v}^* = \arg \max_{\mathbf{v}} E_w \mathbf{I}(\boldsymbol{\theta}) W(\boldsymbol{\theta}; \mathbf{u}; w) \ln h(\boldsymbol{\theta}; \mathbf{v}) \quad (3.10)$$

Equation (3.10) can be solved using a stochastic counter (generating samples with number of simulation N for $\boldsymbol{\theta}$) part of Equation (3.8) to give:

$$\max_{\mathbf{v}} \widehat{\mathcal{D}}(\mathbf{v}) = \max_{\mathbf{v}} \frac{1}{N} \sum_{i=1}^N \mathbf{I}(\theta_i) W(\theta_i; \mathbf{u}; w) \ln h(\theta_i; \mathbf{v}) \quad (3.11)$$

Where, $\theta_1, \dots, \theta_N$ are the random samples generated from $h(\cdot; w)$. Differentiating the function $\widehat{\mathcal{D}}$ in Equation (3.11) with respect to \mathbf{v} , the maximum value is obtained at a point where the derivative is equal to zero.

$$\frac{1}{N} \sum_{i=1}^N \mathbf{I}(\theta_i) W(\theta_i; \mathbf{u}; w) \nabla \ln h(\theta_i; \mathbf{v}) \quad (3.12)$$

Where, the gradient (derivative) is performed with respect to \mathbf{v} (e.g., with respect to μ and σ).

The advantage of this approach is that the solution of Equation (3.12) can be calculated analytically specially if the distributions of the random variables belong to a natural exponential family (Rubinstein, 1997).

Since the objective of the method is to attain estimation of rare-events, Equations (3.11) and (3.12) are performed by constructing a sequence of reference parameters, \mathbf{v}_t and a sequence of levels ($g(\boldsymbol{\theta}) < \gamma_t$), and iterate in both \mathbf{v}_t and γ_t . The goal of this procedure is to converge \mathbf{v}_t to \mathbf{v}^* (μ and σ near the optimal distribution) and γ_t to zero ($g(\boldsymbol{\theta}) \leq 0$, failure) (De Boer et al., 2005 and Botev et al., 2013).

Figure 3.1 summarizes the general procedure of the Cross-entropy method which incorporates the evolution of $h(\boldsymbol{\theta}; \mathbf{u})$ to $h(\boldsymbol{\theta}; \mathbf{v}_t)$ and finally near to $f_{opt}(\boldsymbol{\theta})$. For example, the random vector, $\boldsymbol{\theta}$,

is defined by the initial parametric vector, $\mathbf{v}_0 = \mathbf{u}$ which is a function of μ_0 and σ_0 . Next, we let γ_0 be such that, under the original density $h(\boldsymbol{\theta}; \mathbf{u})$, the intermediate probability level, $P[g(\boldsymbol{\theta}) < \gamma_0] = E_h I_{(g(\boldsymbol{\theta}) \leq \gamma_0)}$, is at least ρ , $\rho \in (0,1)$, for example, $\rho = 0.1$ or 10%. We then update the parametric vector \mathbf{v}_0 to $\mathbf{v}_1 = [\mu_1, \sigma_1]$ defined as the mean and standard deviation of the samples on the 10% intermediate probability level, γ_0 . Then, using μ_1 and σ_1 , a distribution for $h(\boldsymbol{\theta}; \mathbf{v}_1)$ is drawn for a sample size N and the next 10% probability level, γ_1 , on $h(\boldsymbol{\theta}; \mathbf{v}_1)$ is identified and the parametric vector is updated to \mathbf{v}_2 . These steps are repeated with the goal for \mathbf{v}_t to converge to \mathbf{v}^* and γ_t to zero ($g(\boldsymbol{\theta}) \leq 0$, failure) by reducing the Kullback-Leibler distance \mathcal{D} .

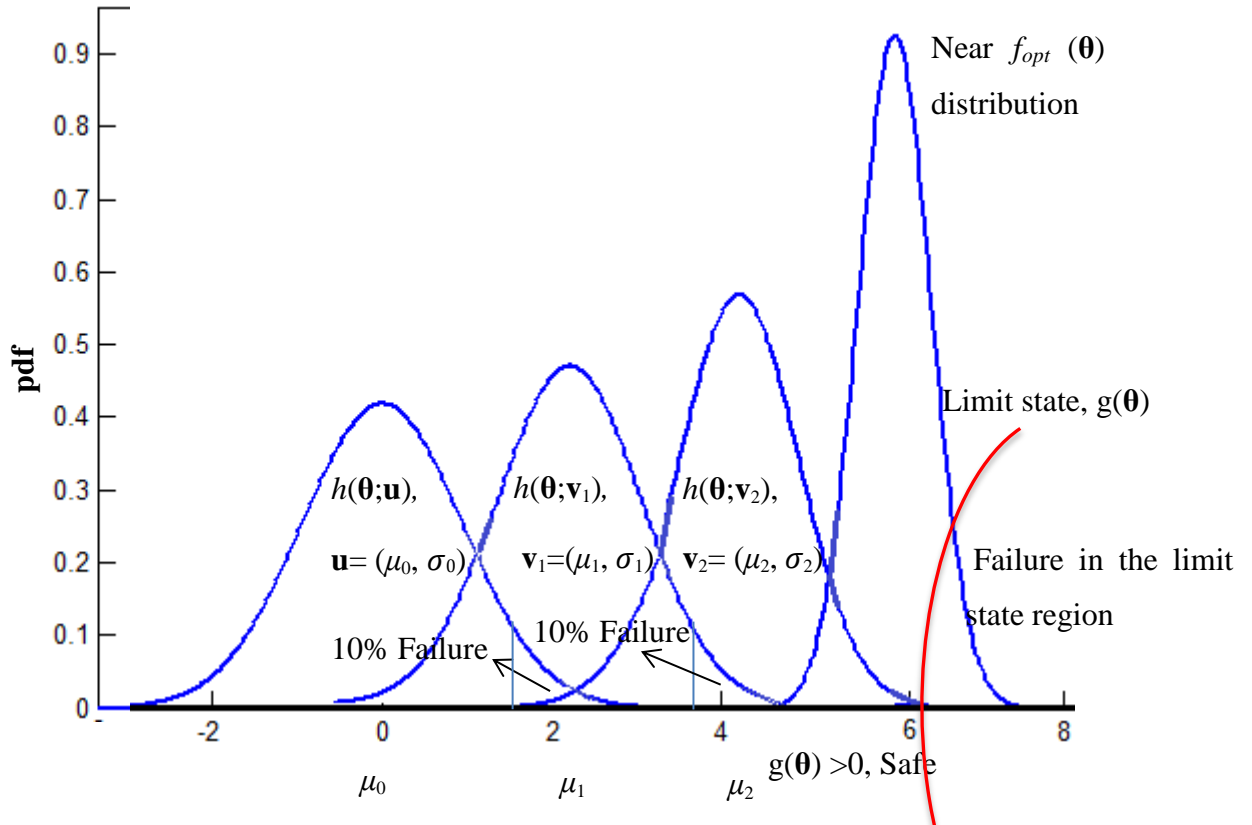


Figure 3.1 Development of the Cross-entropy method for reliability analysis

In other words, each iteration of the algorithm consists of two main phases. In the first phase, γ_t is updated and in the second \mathbf{v}_t is updated. Specifically, starting with $\mathbf{v}_0 = \mathbf{u}$, we obtain the subsequent γ_t and \mathbf{v}_t as follows: (De Boer et al., 2005 and Botev et al., 2013)

- 1. Adaptive updating of γ_t :** For a fixed \mathbf{v}_{t-1} , we first generate N random sample parameters $\theta_i, i= 1, \dots, N$ according to the density function $h(\boldsymbol{\theta}; \mathbf{v}_{t-1})$, then with these trial parameters, we calculate the associated performance function $g(\theta_i), i= 1, \dots, N$. These N values are then sorted in an increasing order $g(\theta_1) \leq \dots \leq g(\theta_N)$. The samples which result in $g(\theta_i) \leq \gamma_t$ are taken as “elites”. Where, γ_t is given by the $\rho N + 1$ or ρ -

quantile value of the sorted values that satisfies the two conditions given by Equations (3.13).

$$P_{\mathbf{v}_{t-1}}(g(\boldsymbol{\theta}) \leq \gamma_t) \leq \rho \quad (3.13)$$

Where, $\boldsymbol{\theta} \sim h(\cdot; \mathbf{v}_{t-1})$.

2. **Adaptive updating of \mathbf{v}_t :** For a fixed \mathbf{v}_{t-1} , derive \mathbf{v}_t from the solution of the CE program as given by Equations (3.11) and (3.12). The optimal solutions of (3.11) and (3.12) can often be obtained analytically, in particular when $h(\boldsymbol{\theta}; \mathbf{v})$ belongs to natural exponential family.

The above rationale results in the following algorithm given by De Boer et al. (2005) for the estimation of probability of failure for rare-events:

Algorithm 1.1: CE Algorithm for Rare-Event Estimation

1. Define $\mathbf{v}_0 = \mathbf{u}$, specify sample size N and ρ . Set $t = 1$ (iteration = level counter).
2. Generate a sample $\theta_1, \dots, \theta_N$ from the density $h(\cdot; \mathbf{v}_{t-1})$ and compute performance function $g(\theta_i)$ and sort in increasing order.
3. Compute γ_t which is the $\rho N + 1$ quantile of the performance function provided $\gamma_t \geq 0$. Otherwise $\gamma_t = 0$.
4. Use the same sample $\theta_1, \dots, \theta_N$ to solve the stochastic program given by Equation (3.11). Denote the solution by \mathbf{v}_t .
5. If $\gamma_t \geq 0$, set $t = t + 1$ and reiterate from step 2. Else proceed with step 6.
6. Estimate the rare-event probability P_f using (3.14)

$$P_f = \frac{1}{N} \sum_{i=1}^N I(\theta_i) W(\theta_i; \mathbf{u}; \mathbf{v}_T) \quad (3.14)$$

Where, T is the final number of iteration.

Smoothed updating: while updating \mathbf{v}_{t-1} to \mathbf{v}_t , instead of updating it directly, a smoothed updating is often performed using $0 \leq \alpha_r \leq 1$ and $0 \leq \beta_r \leq 1$ (De Boer et al., 2005). This will be discussed in Section 3.3.

3.3 Cross-Entropy Method for Optimization

Subsequent work by Rubinstein (1999; 2001) has shown a small modification of the CE algorithm in Rubinstein (1997) can be used to solve optimization problems so that the optimization problems are translated in to rare-event estimation problems.

Suppose the goal is to find the minimum of $C(\mathbf{t})$ over a given space of design variable $\Omega_{\mathbf{t}}$, where \mathbf{t} =design variable = $[t_1, t_2, \dots, t_n] \in \Omega_{\mathbf{t}}$. Assume, for simplicity, there is only one minimizer \mathbf{t}^* . Denote the minimum by γ^* , so that;

$$\min C(\mathbf{t}^*) = \gamma^* \tag{3.15}$$

We can now associate the above optimization problem given by Equation (3.15) with an estimation of the probability $P_f = P(g(\mathbf{t}) \leq 0)$ where, \mathbf{t} has some probability density $h(\mathbf{t}; \mathbf{u})$ on $\Omega_{\mathbf{t}}$ and the unknown γ^* is close to 0. Typically, P_f is a rare-event probability, and the multi-level CE approach of Algorithm 1.1 presented above can be used to find an importance sampling distribution that concentrates all its mass in a neighborhood of the point \mathbf{t}^* . Sampling from such a distribution thus produces optimal or near-optimal states. Note that, in contrast to the rare-event simulation setting, the final level $\gamma^* = 0$ is generally not known in advance, but the CE method for optimization produces a sequence of levels γ_i and reference parameters \mathbf{v}_i such that ideally the former tends to the optimal γ^* and the latter to the optimal reference vector \mathbf{v}^* corresponding to the point mass at \mathbf{t}^* .

Figure 3.2 is a simple illustration between \mathbf{t} and $C(\mathbf{t})$ intended to show and clarify the method of CE optimization with the aim to obtain the minimum $C(\mathbf{t})$. For a given sample size, N of a random design variable, \mathbf{t} , defined by $t_i, i=1, \dots, N$, i.e., $t_i = [t_1, t_2, \dots, t_N]$, the respective values of $C(t_i) = [C_1, C_2, \dots, C_N]$ are calculated at the first step. Similar to Algorithm (1.1), the $\rho N + 1$ quantile is selected to give C_1 and all t_i values which yield $C(t_i) \leq C_1$ are assumed as ‘elites’; therefore, we take $\hat{t}_1 = [t_4, t_6, \dots, t_{13}]$ which gives $C(t_i) \leq C_1$ and a normal distribution I is drawn using mean and standard deviation of \hat{t}_1 to generate N size samples. Using this generated samples, $C(\hat{t}_1)$ is calculated and the respective $\rho N + 1$ quantile is selected to give C_2 . Similarly, we select $\hat{t}_2 = [t_5, t_6, \dots, t_{11}]$ which gives $C(\hat{t}_1) \leq C_2$ and the second normal distribution II is drawn using the mean and standard deviation of \hat{t}_2 to generate N size samples. The same procedure is also repeated on the next iteration where $\hat{t}_3 = [t_5, t_6, t_7]$ are taken as ‘elites’. On this step, the third normal distribution III is narrow in width as compared to the I and II distributions because the standard deviation converges to near zero or zero; therefore, the mean of \hat{t}_3 converges to t_6 and $C(t_6)$ is the minimum point given by point A.

In each iteration the standard deviation is decreased and converges to zero or near zero near at the optimal point (minimum point in this case). The repeated iteration and updating of mean and standard deviation is important to give global minimum (point A) by avoiding local minimum (point B).

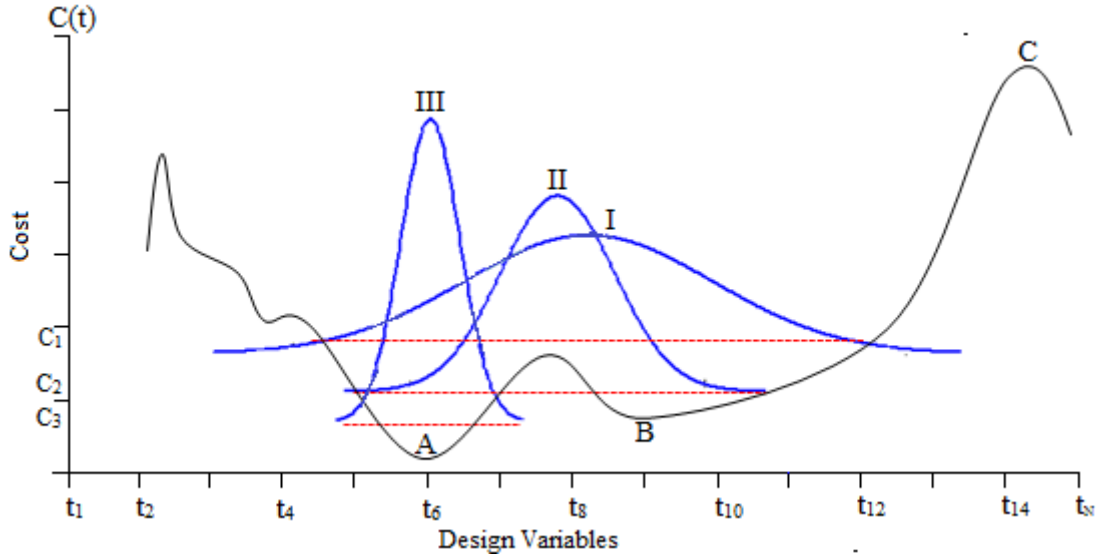


Figure 3.2 Illustration of the CE optimization method

The above discussion on the CE optimization can be summarized by Algorithm 2.1 presented by Rubinstein (1999). The situation is similar to the rare-event simulation of Algorithm 1.1.

Algorithm 2.1: CE Algorithm for Optimization

1. Choose an initial parameter vector, $\mathbf{v}_0 = \mathbf{u}$, specify sample size N and ρ . Set $t = 1$.
2. Generate a sample $t_i, i=1, \dots, N$ from $h(\cdot; \mathbf{v}_{t-1})$ and compute $C(t_i)$ and sort in increasing order.
3. Compute γ_t which is the $\rho N + 1$ quantile of the objective function, $C(t_i)$
4. Use the same sample t_1, \dots, t_N to solve the stochastic program given by Equation (3.11) with $W=1$. Denote the solution by \mathbf{v}_t .

$$\max_{\mathbf{v}} \hat{D}(v) = \max_{\mathbf{v}} \frac{1}{N} \sum_{i=1}^N I(t_i) \ln h(t_i; \mathbf{v}) \tag{3.16}$$

Where, $W=1$ because we are not concerned to calculate P_f and the ratio $h(\mathbf{t}; \mathbf{u}) / h(\cdot; \mathbf{v}_{t-1})$ is ignored.

5. If some stopping criterion is satisfied, stop; otherwise, set $t = t + 1$ and reiterate from step 2.

Smoothed updating: while updating \mathbf{v}_{t-1} to \mathbf{v}_t , instead of updating it directly via Equation (3.10), a smoothed updating is often performed using $0 \leq \alpha_p \leq 1$ and $0 \leq \beta_p \leq 1$ (De Boer et al., 2005). Equation 3.17 gives the updating procedure for the mean and standard deviation of the parametric vector, $\mathbf{v}_t = [\mu_t, \sigma_t]$.

$$\mu_t = \alpha_p \mu_t + (1 - \alpha_p) \mu_{t-1} \quad (3.17a)$$

$$\sigma_t = \beta_p \sigma_t + (1 - \beta_p) \sigma_{t-1} \quad (3.17b)$$

The main reason for using this smoothed updating is to prevent the occurrence of local minima by preventing the occurrence of 0s and 1s in the parameter vectors; once such an entry is 0 or 1, it often will remain so forever, which is undesirable (occurrence of local minima).

4. CE-RBDO Validation on an academic example

4.1 Introduction

The main objective of this chapter is to implement and validate the CE-RBDO algorithm on a problem with an analytical solution. The problem is evaluated for a range of dimensions of the reliability and optimization problems.

Together with implementation of the algorithm, a study on the effects of the updating parameters (α and β), percentage of failure in each iteration (ρ) and number of samples (N) used for simulation have been evaluated. Finally, the results obtained using CE algorithm will be compared with the existing reliability and optimization methods and with the analytical solution.

4.2 Problem Definition

RBDO problems are commonly defined as the minimizations of expected life time costs considering construction and maintenance costs together with the eventual failure (Kupfer and Freudenthal, 1977). Similarly, the RBDO problem given by Equation (4.1) defines the objective function as a function of initial cost, maintenance cost and failure probability.

$$\text{Minimize: } C(\boldsymbol{\theta}, \mathbf{t}) = \sum_{i=1}^n C_i t_i^2 + C_F P_f(\boldsymbol{\theta}, \mathbf{t}) \quad (4.1a)$$

Subjected to

$$P_f(\boldsymbol{\theta}, \mathbf{t}) \leq P_f^{\text{tol}} \quad (4.1b)$$

$$t_{\min} \leq \mathbf{t} \leq t_{\max} \quad (4.1c)$$

Where,

$C(\boldsymbol{\theta}, \mathbf{t})$ is the objective function defined as the loss function (i.e., design cost).

$\boldsymbol{\theta}$ =Random parameters = $[\theta_1, \theta_2, \dots, \theta_d] \in \Omega_{\theta} \subset \mathbf{R}^d$

\mathbf{t} =Design variables = $[t_1, t_2, \dots, t_n] \in \Omega_t \subset \mathbf{R}^n$, Ω_t is the space of design variables.

$C_i(\mathbf{t})$ defines the initial cost of the structure (e.g., material, installation costs).

$C_F(\mathbf{t})$ represents the cost of failure.

$P_f(\boldsymbol{\theta}, \mathbf{t})$ is the failure probability which should be less than the allowable, P_f^{tol} .

$t_{min} \leq \mathbf{t} \leq t_{max}$ shows the boundary condition for the design variable.

Input parameters:

- $C_F=10^{10}\text{€}$
- $\theta_j \sim N(0,1)$, Normally distributed with $\mu_{\theta}=0$ and $\sigma_{\theta}=1$.
- $t_i \sim U(t_{min}, t_{max})$, Uniformly distributed bounded between 0 and 10.
- $P_f^{tol}=10^{-4}$.
- For simplicity $t_1=t_2=t_3\dots, t_n$
- The Reliability problem for estimation of P_f is given by the performance function in Equation (4.2).

$$g(\boldsymbol{\theta}, \mathbf{t}) = \sum_{i=1}^n t_i - \sum_{j=1}^d \theta_j \tag{4.2}$$

Therefore, the Cross-entropy is implemented to solve the reliability and optimization sub-problems within the RBDO problem of Equations (4.1) and (4.2) which will be presented in the next Sections of 4.3 and 4.4 respectively.

4.3 Reliability Analysis using the CE algorithm

Algorithm 1.1 discussed on the previous Chapter of Section 3.2.1 has been implemented to estimate the reliability (probability of failure) for the performance function given in Equation (4.2). The next section will evaluate and discuss the implementation of Algorithm 1.1 in 1D, 2D and higher dimensional problems.

4.3.1 One-dimensional problem (1D)

Equation (4.2) can accommodate wide range of dimensionality based on n and d values. For the case of one-dimensional problem (n=1 and d=1), a single random vector and a design variable is considered. Therefore, a normal random variable, θ , with a zero-mean and unit standard deviation is considered. To evaluate the performance of the CE approach for a rare-event estimation, the design variable is taken equal to 5. Equation (4.3) shows the performance function for the one-dimensional reliability problem.

$$g(\theta, \mathbf{t}) = 5 - \theta \tag{4.3}$$

Failure probability defined as $P_f = P[\theta > 5]$ was to be estimated. Table 4-1 shows the results obtained for the CE method, existing methods (MC and IM) and the analytical solution (from the standard normal table).

Table 4-1 Results of the MC, IM and CE and analytical solution

Simulation Methods	Sample size, N	P_f
Monte Carlo (MC)	500	0
Monte Carlo (MC)	10,000,000	1.000e-07
Importance Sampling (IM)	500	2.982e-07
Cross-entropy (CE)	500	2.943e-07
Standard Table		2.870e-07

As it can be seen from Table 4-1, the simulation of the one-dimensional problem using the CE algorithm gave good convergence with the analytical solution. Moreover, the number of samples used for the simulation were quite less when compared to the MC method which required over 10^6 samples. As discussed in Chapter 2, the IM requires knowledge of the design point to provide an efficient estimate of P_f . In this case the design point is defined as $\theta=5$. Therefore, the IM method also resulted in an accurate estimate of probability of failure when compared to the standard normal table and CE.

4.3.2 Two-dimensional (2D) and higher dimensional Problems

The algorithm used to solve the one-dimensional problem was examined on high dimensional problems. In this section the implementation and validation of the algorithm will be examined together with the investigation on the effects of α_r , β_r , ρ and N on the performance of the approach. The results based on the CE implementation will be compared with the analytical solution. The procedures followed to solve the reliability problem are presented for both the analytical and the CE algorithm methods.

Analytical Solution

The analytically solution for Equation (4.2) can be obtained for a given \mathbf{t} value denoted by $\mathbf{t}^* = [t_1^*, \dots, t_n^*]$. From discussion in Section 2.2.2(A) of Equation (2.13), the mean and standard deviation of the performance function can be calculated as:

$$\mu_g = \mathbf{E}(g) = \sum_{i=1}^n t_i^* - \sum_{i=1}^d \mu_{\theta_j} = \sum_{i=1}^n t_i^* - d \mu_{\theta_j} \tag{4.4}$$

$$\sigma_g = \sqrt{\text{Var}[g]} = \sqrt{\sum_{j=1}^d \left(\frac{\partial g}{\partial \theta_j}\right)^2 \sigma_{\theta_j}^2} = \sigma_{\theta_j} \sqrt{d} \tag{4.5}$$

Therefore, substituting the given mean ($\mu_{\theta} = 0$) and standard deviation ($\sigma_{\theta} = 1$) of the random variable, θ , in to Equations (4.4) and (4.5), the reliability index is calculated as: $\beta = \frac{\mu_g}{\sigma_g}$ and

the estimate of the failure probability is analytically calculated under the assumption that g is normally distributed: $P_f = 1 - \varphi(\beta) = \varphi(-\beta)$. This gives a direct relation between β and summation of \mathbf{t}^* so that for a given \mathbf{t} value denoted by $\mathbf{t}^* = [t_1^*, \dots, t_n^*]$, the corresponding β and P_f can be estimated.

To evaluate the performance of the CE approach for a rare-event estimation, β is fixed to 4 and the corresponding $P_f = 3.161712 \times 10^{-5}$. Moreover, the design point, $\mathbf{t}^* = \frac{4\sqrt{d}}{n}$, can be obtain using $\beta = 4$ and Equations (4.4) and (4.5).

CE approach Solution

The procedures described in Algorithm 1.1 were followed to estimate the probability of failure for the different combinations of n and d that extend from two-dimensional to higher dimensions. The following section will present the general results obtained using the Cross-entropy algorithm and discuss effects of the different parameters (α_r , β_r , ρ and N).

A. Results for Two dimensional (2D) Problem (n=2 and d=2)

Table 4.2 shows the results obtained using the CE algorithm for $n=2$, $d=2$ and $\rho=0.1$ with different α_r , β_r and N . By comparison of the results with the analytical solution given above, $P_f = 3.161712 \times 10^{-5}$ and $\beta = 4$, the study on the updating parameters α_r and β_r show the choice of α_r does not have a significant effect on the final result while β_r between 0.5 and 1 leads to an accurate estimate. Lower β_r values resulted in a slight deviation of the probability of failure from the true value and were found to be time consuming because the number of iterations, T ,

was relatively higher; therefore, $\alpha=1$ and $\beta_r=0.7$ will be used for further study on high dimensions ($n>2$ and $d>2$).

The effect of the sample sizes were also studied such that the sample sizes $N=100, 300$ and 800 were used. As can be seen in Table 4-2, the efficiency of the CE method to estimate P_f improved as the sample size increased. $N=100$ was found to be sufficient to provide a good estimate of P_f with a relatively less computational time. **Note:** β_r = updating parameter and β = reliability index.

Table 4-2 Estimation of P_f for $n=2, d=2$ and $\rho =0.1$ with variable α_r, β_r , and N

α_r	β_r	N=100			N=300			N=800		
		T	P_f	β	T	P_f	β	T	P_f	β
1	1	4	3.010e-05	4.0120	4	3.193e-05	3.9989	4	3.182e-05	3.9975
1	1	4	2.913e-05	4.0197	4	3.209e-05	3.9969	4	3.109e-05	4.0040
0.5	1	4	3.872e-05	4.1228	4	3.087e-05	4.0061	5	3.471e-05	3.9782
0.5	1	4	3.635e-05	3.9673	4	3.411e-05	3.9824	4	2.608e-05	4.0463
0.2	1	4	3.273e-05	3.9286	6	2.202e-05	4.0852	5	3.317e-05	3.9890
0.2	1	4	2.798e-05	4.0293	5	2.501e-05	4.0556	6	3.077e-05	4.0070
1	0.5	4	2.286e-05	4.0765	4	3.483e-05	3.9826	5	3.036e-05	4.0090
1	0.5	4	3.891e-05	3.9510	5	3.387e-05	3.9774	5	3.488e-05	3.9784
1	0.2	6	1.798e-05	4.1320	6	2.057e-05	4.1009	6	4.731e-05	3.9040
1	0.2	7	2.243e-05	4.0809	6	2.141e-05	4.0428	6	2.010e-05	4.1063
0.5	0.5	5	5.212e-05	3.8008	6	3.921e-05	3.9492	6	2.896e-05	4.0211
0.5	0.5	4	2.181e-05	4.0874	6	3.406e-05	3.9828	6	2.918e-05	4.0193

Figures 4.1 and 4.2 illustrates the propagation of the generated samples in each iteration from the initial point [0,0] to the design point [2.8285, 2.8285]. These figures show the methodology followed by the CE method as discussed in Chapter 3.

$\alpha_r=1, \beta_r=0.7, N=800$ and variable ρ have been used in this case to evaluate the effect of ρ . The use of $\rho=0.01, 0.05, 0.1$ and 0.4 was assessed such that, in case of $\rho=0.4$, almost half of the previous samples were used to generate the next distribution which resulted in a relatively higher computational time as compared to lesser ρ values, otherwise, the use of $\rho=0.01, 0.05, 0.1$ and 0.4 showed accurate convergence of the random numbers, θ_1 and θ_2 , from the origin to the intended design point.

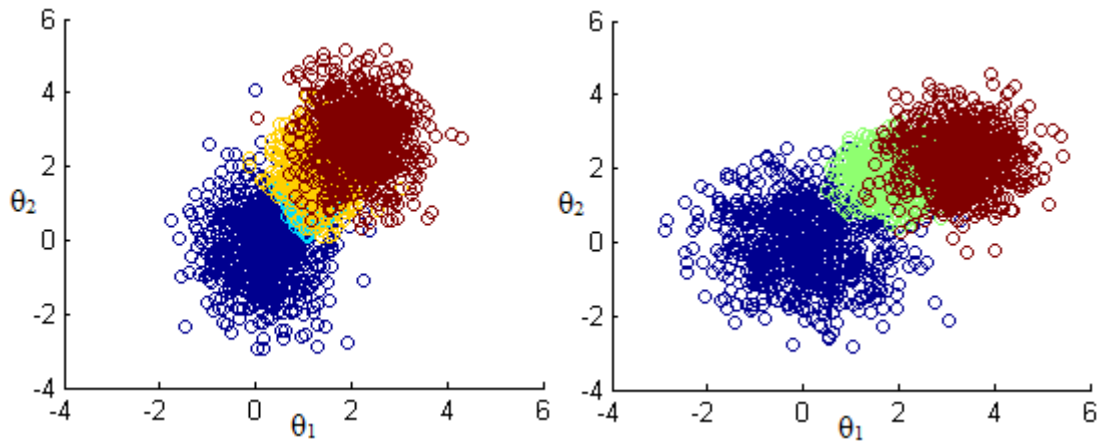


Figure 4.1 Plot for $\rho=0.01$ (left) and $\rho=0.05$ (right) with $N=800$

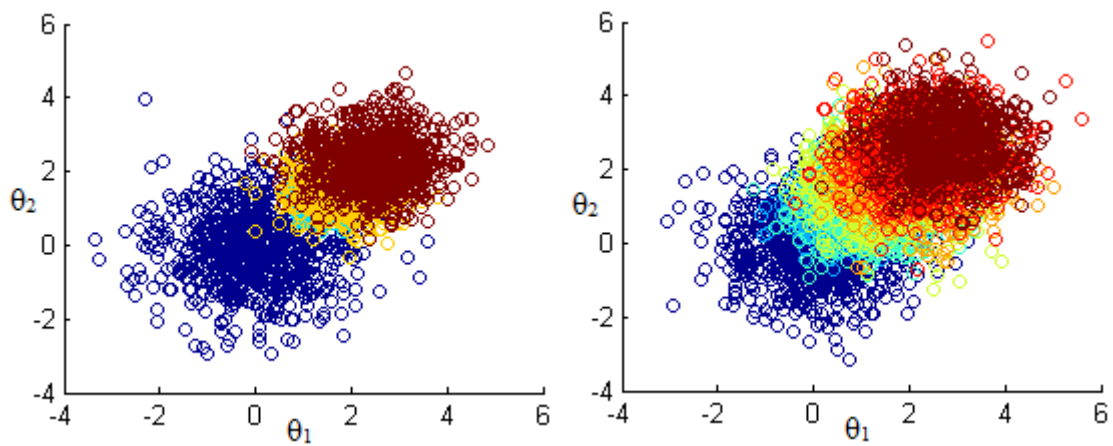


Figure 4.2 Plot for $\rho=0.1$ (left) and $\rho=0.4$ (right) with $N=800$

Figure 4.3 also shows the propagation of the samples from safe region ($g(\boldsymbol{\theta}) > 0$) to the failure region for $\alpha_r=1$, $\beta_r=0.7$, $\rho=0.1$ and $N=800$ with the iteration, T . The convergence to failure, $g(\boldsymbol{\theta}) < 0$, was obtained in the fourth iteration as can be seen in two (2D) and three (3D) dimensional views. The performance function gave $g(\boldsymbol{\theta}) > 2$ for all samples ($N=800$) in the first iteration which shows the safe region while in the fourth iteration, some samples yield $g(\boldsymbol{\theta}) < 0$.

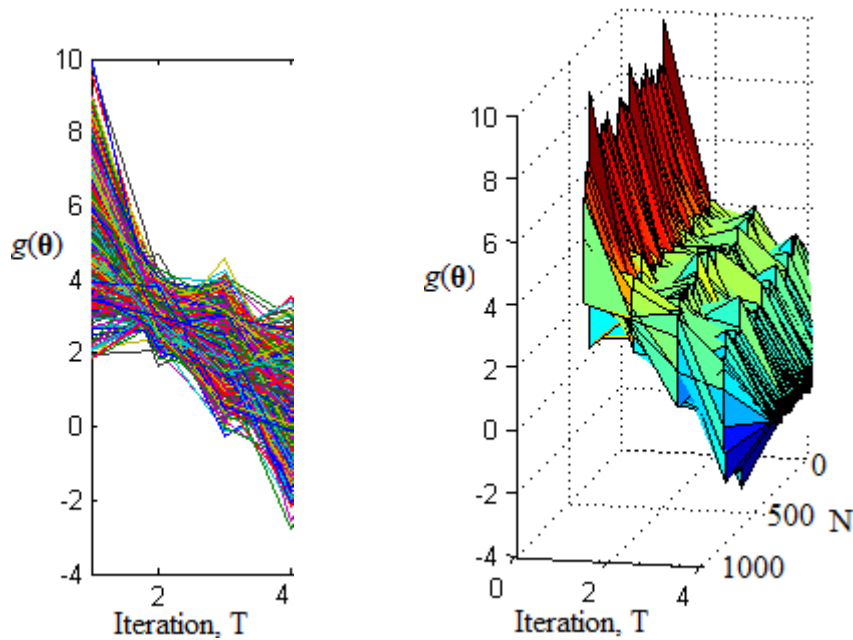


Figure 4.3 Illustration of 2D (left) and 3D (right) view for convergence of $g(\theta)$

B. Results for High dimensional Problems up to $n=100$ and $d=100$

The study on $n=2$ and $d=2$ was extended further to solve high dimensional problems. Table 4.3 shows the results obtained for $(n=5, d=5)$, $(n=10, d=10)$ and $(n=20, d=20)$ for different ρ and N . Unlike to the discussion earlier for $n=2$ and $d=2$, the estimation of the probability of failure became unstable for lower sample size ($N=100$) and even provided poor estimation for high n and d values (e.g. $n=20$ and $d=20$); therefore, as can be seen in the Table 4.3, the increase from $N=100$ to 500 (for $n=10, d=10$) and 1500 (for $n=20, d=20$) resulted in a better estimate of P_f .

The study on ρ showed that the choice in ρ value does not have significant effect on P_f or β for n and m values less than 10 except for some lower values ($\rho=0.01$) and small sample sizes ($N=100$), but, for the high dimensional ($n=20, d=20$) analysis, it was observed that lower ρ values resulted in unstable results which also deviated from the analytical solution as can be seen in Table 4-3. Therefore, it can be concluded from Tables 4-2 and 4-3, high dimensional problems require larger sample size, N , and ρ than low dimensional problems. The main reason for this can be explained as; the increase in the dimensionality requires large sample sizes and ρ to simulate the region of the joint distribution of the random vectors (large number uncertain parameters).

Table 4-3 Estimation for (n=5, d=5), (n=10, d=10) and (n=20, d=20)

N	ρ	n=5, d=5			n=10, d=10		n=20, d=20	
		T	P_f	β	P_f	β	P_f	β
100	0.1	4	3.42e-05	3.9816	9.02e-05	3.7453	5.46e-07	4.8742
		4	1.20e-05	4.2231	2.31e-05	4.0724	1.60e-07	5.1109
500	0.1	4	3.33e-05	3.9885	2.64e-05	4.0431	3.35e-05	3.9864
		4	3.49e-05	3.9769	2.82e-05	4.0271	4.43e-07	4.9154
1500	0.1	4	3.06e-05	4.0081	2.35e-05	4.0705	2.35e-05	4.0701
		4	2.98e-05	4.0147	3.26e-05	3.9935	2.744e-05	4.0343

For further evaluation on the CE method, $\rho=0.3$ and $\rho=0.4$ were used and their effect have been studied together with the effect of using N=100, 500 and 1500. Table 4-4 shows the reliability analysis for a high dimensional problem of n=60 and d=60. It can be seen lower N, N=100 and 500, yielded unstable results while acceptable results are obtained when $\rho=0.4$ and N=1500 although the number of iterations (T=11) is increased considerably. (Refer Figure 4.4 for comparison of the results in terms of reliability index values, β obtained from Table 4-4).

Table 4-4 Estimation of P_f for n= 60 and d=60

N	$\rho = 0.3$			$\rho = 0.4$		
	T	P_f	β	T	P_f	β
100	7	2.244e-10	6.2360	7	2.923e-09	5.8211
	7	1.041e-07	5.1917	7	2.448e-10	6.2224
500	7	2.662e-06	4.5516	9	5.725e-06	4.3878
	7	6.946e-06	4.3455	9	6.967e-06	4.3449
1500	8	1.645e-05	4.1524	11	3.769e-05	3.9559
	8	3.130e-06	4.5174	11	3.140e-05	4.0020

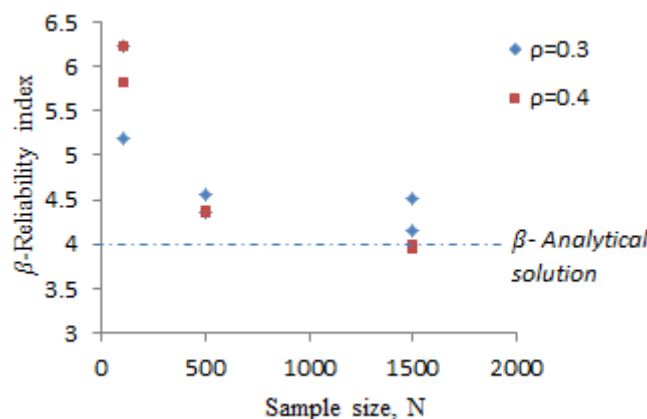


Figure 4.4 Estimation of P_f or β for n= 50, d=50 for $\rho=0.3$ and $\rho=0.4$

Further study on a high dimensional n>60 and d>60 problem gave unstable results demonstrating the limitation of the CE algorithm.

4.3.3 Comparison of the CE algorithm results with existing methods

From the discussion in Section 4.3.2, the reliability analysis problem with $n=2$, $d=2$ and $\rho=0.1$ was selected and the result based on the CE algorithm is compared with the Monte Carlo (MC), Importance Sampling (IM), Subset Simulation (SS) and the analytical solution as presented in Table 4-5. As discussed in Chapter 2 and Section 4.3.1 of this chapter, the MC simulation can be inefficient for low P_f . Similarly on this case, $N=1,000,000$ is required to get a reasonable estimate of P_f which was found to be computationally demanding.

For case of IM, the design point should be known a priori to give a good estimate of P_f in which it has been estimated to be $[2.8285, 2.8285]$ in this particular case for 2D. The SS also gave good estimation of probability of failure with $N=100$ similar to the CE method as can be seen in Table 4-5. The CE required four iterations while the SS was simulated six times. It can be concluded for this particular case, the CE method performed well both in accuracy and efficiency.

Table 4-5 Comparison of the CE method with other existing methods

Reliability analysis Method	N	P_f
MC (Monte Carlo)	1000000	2.800e-05
IM (Importance Sampling)	100	3.307e-05
SS (Subset Simulation)	6x100	2.500e-05
CE (Cross Entropy)	4x100	2.891e-05
Analytical (True) Solution		3.162e-05

4.3.4 Discussion and Summary on reliability analysis

From the above study and validation of the CE method for the reliability analysis (estimation of P_f) on the 1D, 2D and high dimensional problems with an analytical solution, the following important findings can be summarized and concluded.

- The study on the updating parameters α_r and β_r showed the choice of α_r does not have a significant effect on the final result while β_r between 0.5 and 1 leads to accurate estimate. Lower β_r values resulted in a slight deviation of the probability of failure from the true value and were found to be time consuming (high number of iteration); therefore, $\alpha_r=1$ and $\beta_r=0.7$ have been selected for further study.
- For problems with $n=(10-20)$ and $d=(10-20)$, increase in the sample size was required and change from $N=100$ to 1500 yielded good estimate of P_f .

- For problems with $n=(20-60)$ and $d=(20-60)$, the use of $\rho=0.1$ did not yield accurate estimates ;therefore, it was increased to $\rho=0.4$ and together with $N=1500$, it gave good estimate of P_f .
- Finally, the method resulted in unstable estimate of P_f for higher dimensional problems $n>60$ and $d>60$. The samples generated for simulation on the joint probability of the random vectors could not perform well demonstrating the limit of the algorithm.
- Comparison of the results obtained using the CE and other existing reliability analysis methods on a 2D performance function showed the CE algorithm resulted in both accuracy and efficiency, that is, it resulted in a good estimate of P_f and required less computational time as compared to both MC and SS.

4.4 Optimization Analysis using CE method

Subsequent work by Rubinstein (1999; 2001) has shown a small modification of the CE algorithm in Rubinstein (1997) can be used to solve optimization problems by translating the optimization problems in to rare-event estimation problems. Therefore, the optimization part of the RBDO problem defined by Equation (4.1) can be solved using the implementation of Algorithm 2.1 and compared to an analytical solution.

Input parameters to solve Equation (4.1) given in Section 4.2 (Problem definition):

- $C_F=10^{10}\text{€}$
- $\theta_j \sim N(0,1)$, Normally distributed with $\mu_{\theta}=0$ and $\sigma_{\theta}=1$.
- $t_i \sim U(t_{\min}, t_{\max})$, Uniformly distributed bounded between 0 and 10.
- $P_f^{\text{tol}}=10^{-4}$.
- For simplicity $t_1=t_2= t_3 \dots, t_n$

Analytical solution procedure

From the reliability analysis discussion in Section 4.3, the reliability index for the performance function, $g(\boldsymbol{\theta})$, is given by:

$$\beta = \frac{\mu_g}{\sigma_g} = \frac{\sum_{i=1}^n t_i - d \mu_{\theta_j}}{\sigma_{\theta_j} \sqrt{d}} \tag{4.6}$$

Substituting the input parameters and taking $t_1=t_2= t_3 \dots, t_n$, Equation (4.6) can be reduced to:

$$\beta = \frac{n t_1}{\sqrt{d}} \quad (4.7)$$

The optimization part of the RBDO problem is concerned with minimizing the objective function, $C(\boldsymbol{\theta}, \mathbf{t})$; therefore, the mathematical derivative of the objective function with respect to t_i gives the values of t_i which result in the minimum or optimal $C(\boldsymbol{\theta}, \mathbf{t})$. The derivative is given by Equation (4.8) and the corresponding t_i value which yield the minimum $C(\boldsymbol{\theta}, \mathbf{t})$ is denoted as $t_{i,\min}$ in Equation (4.9).

$$\frac{\partial C}{\partial t_i} = 0 \quad (4.8)$$

$$t_{i,\min} = \frac{C_F}{2C_i \sqrt{d}} \phi(-\beta) \quad (4.9)$$

Where $\phi(-\beta)$ is the pdf (probability distribution) which is the derivative of the cumulative distribution function, $\Phi(-\beta)$ given by:

$$\phi(-\beta) = \frac{1}{\sqrt{2\pi}} \exp\left(-\frac{1}{2}(-\beta)^2\right) \quad (4.10)$$

By rearranging Equation (4.9), the initial cost, C_i can be defined interms of $t_{i,\min}$. This is shown by Equation(4.11) as:

$$C_i = \frac{C_F}{2 t_{i,\min} \sqrt{d}} \phi(-\beta) \quad (4.11)$$

Finally, the analytical solution can be obtained by equating $t_i = t_{i,\min}$ on Equations (4.7) and (4.9). For a given β and the dimensionality denoted by n and d , the Equations from (4.6) to (4.11) are used to give analytical solution of the problem in Equation (4.7).

CE algorithm solution

This portion discusses the preparation of the CE algorithm to solve the optimization sub-problem within the RBDO problem given by Equation (4.1). The input parameters includes: n , d , ρ , β (reliability index), the updating parameters for optimization (α_p and β_p) and sample size (N). It is recommended to refer back to Algorithm 2.1 and Figure 3.2 for the discussion below.

A uniform distribution of t_i bounded between 0 and 10 were initially generated as given by Equation (4.1c), $t_i \sim U(t_{\min}, t_{\max})$. These generated samples have been used to estimate the failure probabilities, P_f , and checked for $P_f < P_f^{\text{tol}}$ as given by Equation (4.1b). Those t_i values

which yield acceptable P_f have been further used for estimation of the cost, $C(\boldsymbol{\theta}, t_i)$ and were arranged in increasing order. As given in step 3 of Algorithm 2.1, the $\rho N+1$ quantile of the sorted $C(\boldsymbol{\theta}, t_i)$ was identified and denoted as γ_t .

All t_i values which yield $C(\boldsymbol{\theta}, t_i) < \gamma_t$ were identified and their mean (μ_t) and standard deviation (σ_t) were calculated. These μ_t and σ_t were updated using the updating parameters α_p and β_p in order to yield fast convergence. Then, using this new mean and standard deviation of t_i , a new distribution of t_i was generated with a sample size of N . The procedures explained above were then repeated until the mean of t_i converged and gave the design cost (C_{\min}).

The next section will present the results obtained using the CE algorithm and the results will be compared with the analytical solution and an existing optimization method (Simulated annealing). Different n and d sizes have been used to consider the high dimensional problems. Moreover, the effects of the updating parameters (α_p and β_p), the sample size (N) and percentage of failure in each iteration (ρ) will be evaluated.

4.4.1 Results for Two-dimensional ($n=2$ and $d=2$) optimization analysis

Given $n=2$, $d=2$ and reliability index, $\beta=4$, the analytical solution can be solved using Equations (4.6) to (4.11), for example, the design point or $t_{i,\min}$ can be obtained to be $t_1=t_2=2.8285$. The cost estimation was performed for different combinations of α_p , β_p and N . Since the cost minimization problem requires the estimation of probability of failure, CE algorithm was performed for two sets of sample sizes. A sample size, $N=100$ have been used for calculation of probability of failure (in Algorithm 1.1) together with $\alpha_r=1$ and $\beta_r=0.7$ and the same sample size have been used initially for the generation of design variables, \mathbf{t} , in Algorithm 2.1.

The use of sample size of $N=100$ together with different combination of updating parameters for reliability (α_r and β_r) and optimization (α_p and β_p) showed deviation on the minimum cost C_{\min} obtained using CE as compared to the analytical solution. The main reason for the deviation was identified to be lack of consistency in calculating the P_f . To reduce this effect higher sample sizes; $N=200, 500, 1000, 1500$ and 2000 were used for calculation of probability of failure (generation of random vectors, $\boldsymbol{\theta}$, in Algorithm 1.1) while the sample size used for generation of design variables, \mathbf{t} , was fixed to $N=100$ (in Algorithm 2.1).

Table 4-6 summarizes the results obtained using CE, Simulated annealing and compared to the analytical solution. Algorithm 1.1 was implemented for the reliability analysis with $\alpha_r=1$, $\beta_r=0.7$ and $\rho=0.1$ and different sample sizes N . For the optimization part, Algorithm 2.1 with

$N=100$, $\alpha_p=0.98$ and $\beta_p=0.98$ was implemented. The CE algorithm was run 10 times and the average results are shown in Table 4-6.

Table 4-6 Comparison of Algorithm solution with Analytical solution

Method	Sample size, N	t_1	t_2	C_{min}
CE	100	2.7405	2.7673	2.6685e+06
	200	2.7947	2.7748	2.8144e+06
	500	2.7936	2.8009	2.8915e+06
	1000	2.8307	2.7982	2.9208e+06
	1500	2.8291	2.8195	2.9420e+06
	2000	2.8267	2.8164	2.9536e+06
Simulated annealing		2.8590	2.859090	2.9592e+06
Analytical solution		2.8282	2.8282	2.9921e+06

As can be seen from Table 4-6, the accuracy of the CE method increased as the sample size N increased from 100 to 2000. Generally, the Cross-entropy method gave good estimate of the minimum cost similar to the results obtained based on an analytical solution and the existing optimization method called Simulated annealing.

The observations on the effects of α_p and β_p can be summarized as; choice of α_p have no significant effect on the final result of the minimum cost while the choice of β_p is significant in which lower values were found to be computationally intensive.

The result from Table 4-6 can be seen as a $\ln(C(\theta, t))$ plot on Figure 4.5 illustrating the minimum design cost, C_{min} , which is equal to $\ln(C) = 14.88$. The design points, $t_1=t_2=2.8285$, which resulted on the design cost, C_{min} , can also be seen in the contour plot given by Figure 4.6 for $\ln(C)$ versus t_1 and t_2 .

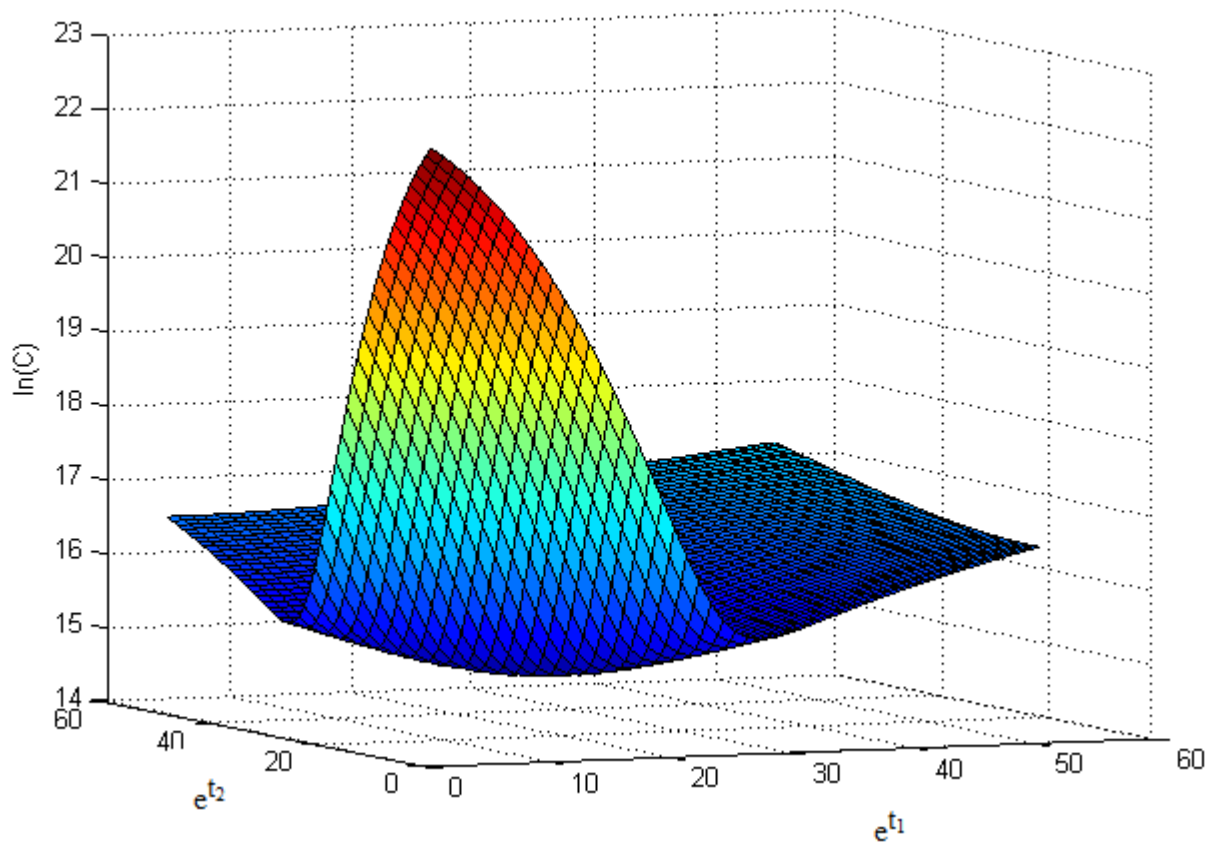


Figure 4.5 ln-plot of Cost for e^{t1} and e^{t2}

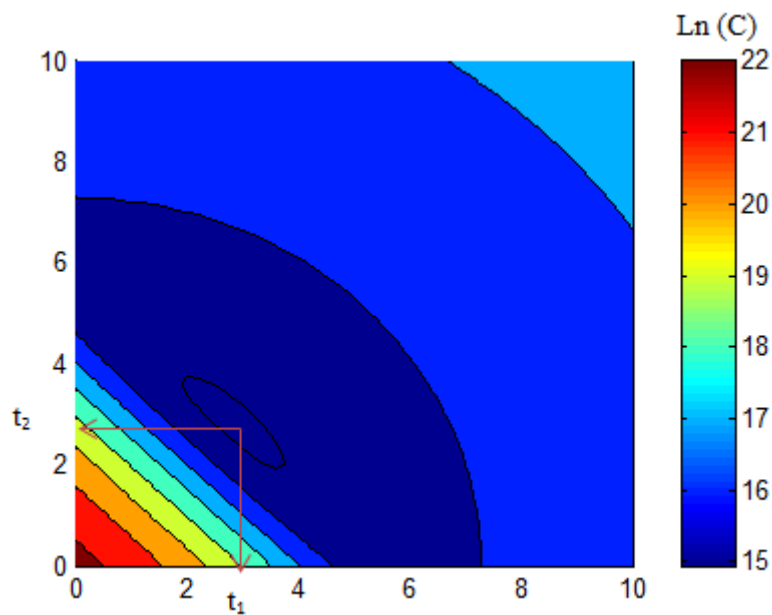


Figure 4.6 Contour plotting of $\ln(C)$ over t_1 and t_2

The optimization tool used for comparison with the CE method is Simulated annealing in which the basics of the method have been already discussed in the literature review. The results obtained using this method can be seen from Figure 4.7 or Table 4-6 as the design points $[2.8590, 2.8590]$ gave a design cost, $C_{\min}=2.9592e+06$.

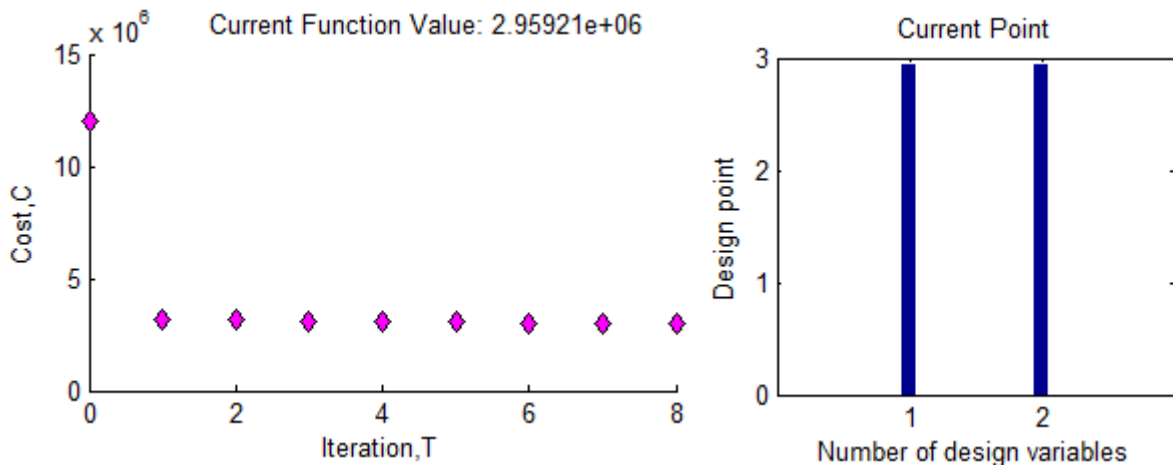


Figure 4.7 Estimation of C_{min} and respective design points from Simulated annealing

4.4.2 Results for high dimensions ($n > 2$ and $d > 2$) optimization analysis

This section will assess the suitability of the CE method to solve $n > 2$ and $d > 2$ optimization problems and further study the limit of the CE algorithm.

Similar to the discussion in Section 4.4.1, the main aim was to solve the objective function given by Equation (4.1a) and all the procedures used to develop the algorithm were the same as the discussion in Section 4.4.1. But, since this section is aiming to simulate high dimensional problems, N and ρ have been increased to yield good estimations. Therefore, $\alpha_r=1$, $\beta_r=0.7$, $N=500$ and $\rho=0.2$ have been used for the calculation of P_f (using Algorithm 1.1) for $n \leq 20$ and $d \leq 20$ while $\alpha_p=0.98$, $\beta_p=0.98$, $N=100$ and $\rho=0.1$ have been used for the optimization of the minimum cost (using Algorithm 2.1). For high dimensions of $n=30$ and $d=30$; $\alpha_r=1$, $\beta_r=0.7$, $N=1500$ and $\rho=0.4$ (in Algorithm 1.1).

Table 4-7 gives the results of minimum cost for the different combinations of n and d . The Cross-entropy method performed well for $n \leq 20$ and $d \leq 20$ while the minimum cost estimated is considerably lower than the true estimate for case of $n=30$ and $d=30$. This can demonstrate the limitation of the CE method.

Table 4-7 High dimensional optimization problems compared with the analytical solution

n	m	C_{min}	C (analytical)
2	2	2.8915e+06	2.9921e+06
2	5	2.8413e+06	2.9921e+06
5	5	2.9146e+06	2.9921e+06
5	2	2.9108e+06	2.9921e+06
10	10	2.8998e+06	2.9921e+06
20	20	2.6948e+06	2.9921e+06
30	30	2.2298e+06	2.9921e+06

4.4.3 Discussion and Summary on optimization analysis

From the above study and evaluation of the CE method to solve the optimization sub-problem within RBDO problems for 2D and high dimensional, the following important findings can be summarized and concluded.

- Since the final (design) cost was defined as a function of initial cost, maintenance cost and probability of failure, consistency in the estimate of P_f was found to be critical; therefore, the sample size was increased to get a good estimation. For the two-dimensional problem, the sample size increased from $N=100$ to 200, 500 and 2000 and resulted in a good estimate of the final cost close to the analytical (true) solution. The computation time increased as the sample size increased but better accuracy was achieved.
- The study on the updating parameters showed selection of α_p have not resulted in a significant change in the estimation of the final cost while it was observed the choice of β_p is significant in which lower values of β_p (<0.5) resulted in a time consuming computation although the final cost is not affected.
- For higher dimensions ($n \leq 20$ and $d \leq 20$), $\alpha_r=1$, $\beta_r=0.7$, $N=500$ and $\rho=0.2$ were used for calculation of P_f (using Algorithm 1.1) while $\alpha_p=0.98$, $\beta_p=0.98$, $N=100$ and $\rho=0.1$ were used for the optimization of the minimum cost (using Algorithm 2.1) to yield a good estimate of the final cost.
- For $n=30$ and $d=30$, the estimation of the final cost gave considerably lower than the true solution although $N=1500$ and $\rho=0.4$ were used. This may be because the algorithm cannot simulate the joint probability distribution for high dimensional problems which show the limit of the CE algorithm.

5. Reliability-Based Design of a Monopile Foundation

5.1 Introduction

Monopiles are mainly used as a foundation for offshore wind turbines in which both wind and wave forces generate significant amount of lateral loads (H) and moments (M). These monopile foundations are made of an open-ended circular steel pile with diameters (D) of 4 to 6 m and embedded pile lengths (L) of 15 to 30 m (LeBlanc, 2009). For attaining stability of the monopile foundation, the lateral loads are absorbed by the pile structure via bending moment and transferred laterally to the soil. In current practices, these piles are commonly designed with the p-y method which is used to determine the lateral soil resistance.

The Det Norske Veritas (DNV, 2004) and American Petroleum Institute (API, 2000) design standards for offshore wind turbine structures use the subgrade reaction approach which employs the p-y curve method for determining the lateral soil resistance. This method is based on the Winkler soil model which replaces the elastic soil medium with a series of infinitely closely spaced independent (uncoupled) springs with stiffness E_{py} as shown on Figure 5.1.

The p-y curves give the relation between the integral values of the mobilized resistance from the surrounding soil, p , when the pile deflects a distance y laterally. The ratio between p and y is used to denote the soil stiffness, E_{py} (DNV, 2004). The solution of pile displacements and pile stresses at any point along the pile for any applied load at the pile head gives the solution to the differential equation of the pile given by Equation (5.1).

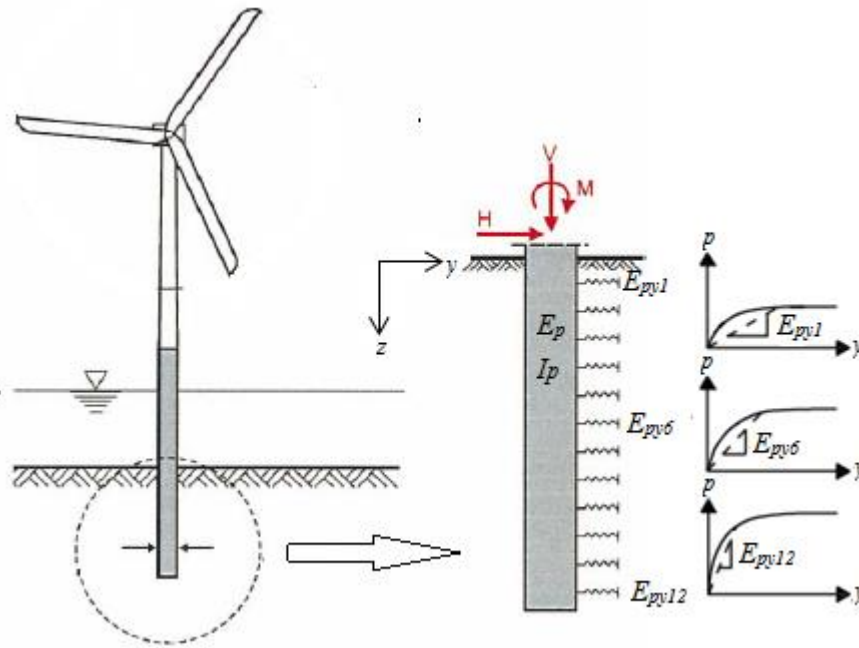


Figure 5.1 Winkler approach with the pile modelled as an elastic beam supported by nonlinear and coupled springs (Bekken, 2009)

Equation (5.1) was developed by Timoshenko (1941) to evaluate the deflection of beams, y . The equation for an infinitesimal small element, dz , located at depth z , with Young's modulus E_p and moment of inertia I_p of a monopile subjected to a lateral loading, can be derived from the static equilibrium given by:

$$E_p I_p \frac{d^4 y}{dz^4} + V \frac{d^2 y}{dz^2} - p(y) = 0 \tag{5.1a}$$

With

$$E_p I_p \frac{d^3 y}{dz^3} + V \frac{dy}{dz} = H \quad \text{and} \quad E_p I_p \frac{d^2 y}{dz^2} = M \tag{5.1b}$$

$$p(y) = E_{py} y \tag{5.1c}$$

- Where, $E_p I_p$ Flexural rigidity of the pile (kNm^2)
- y Pile lateral deflection at any point z along the pile (m)
- $p(y)$ Soil reaction per unit length (kPa) given by Equation (5.1c)
- H Lateral load (kN) on the pile at position z
- V Axial load (kN) on the pile at position z and
- M Bending moment (kNm) on the pile at position z

To solve Equation (5.1a), the $p(y)$ defined as the soil reaction per unit length should be initially estimated. For this particular study, the soil type is given as *stiff clay under water* with *static* loading. The stiff clay is defined by undrained shear strength, S_u and soil submerged unit weight, γ' ; therefore, API (2000) provides the general procedures to follow to estimate the p - y curve or $p(y)$ and the respective E_{py} ;

1-Obtain values of the undrained shear strength, S_u (will be discuss in detail on the next sections), soil submerged unit weight, γ' , and the pile diameter, D .

2-Compute the average undrained shear strength $S_{u,mean}$, over depth, z .

3-Compute the ultimate soil resistance per unit length of pile (p_u) using the smaller of the values given by Equation (5.2) as:

$$p_u = 2S_u D + \gamma' D z + 2.83 S_u z \quad \text{or} \quad p_u = 11 S_u D \quad (5.2)$$

4-Choose appropriate static loading coefficient, A_s , for the particular non-dimensional depth (z/D). If $z/D \geq 3.5$, $A_s = 6$, otherwise Equation (5.3) is used.

$$A_s = -0.0011 \left(\frac{z}{D}\right)^4 + 0.0193 \left(\frac{z}{D}\right)^3 - 0.1223 \left(\frac{z}{D}\right)^2 + 0.3532 \left(\frac{z}{D}\right) + 0.2 \quad (5.3)$$

5-Establish the initial straight-line portion of the p - y curve as given by Equation (5.4)

$$p = (k_s z) y = E_{py} y \quad (5.4)$$

Choose the value of $k_s = E_{py}/z$, variation of soil reaction modulus over depth, from Table 5-1.

Table 5-1 Representative of k_s for overconsolidated clay (API, 2000)

$S_{u, mean}$ (kPa)	50-100	100-200	300-400
k_s (MN/m ³)	135	270	540

6-Calculate the deflection at $0.5p_u$ denoted by y_{50} : $y_{50} = \epsilon_{50} D$ (5.5)

Use the appropriate values of ϵ_{50} (strain at $S_{u, mean}$) from results of laboratory tests or in the absence of laboratory tests, from Table 5-2.

Table 5-2 Representative of ϵ_{50} for overconsolidated clay (API, 2000)

$S_{u, mean}$	50-100	100-200	300-400
ϵ_{50}	0.007	0.005	0.004

7-Calculation of soil resistance, p , is given by Equations (5.6) to (5.9) as: (API, 2000)

$$\text{For } (y/y_{50} \leq A_s) : p = 0.5 p_u (y/y_{50})^{0.5} \quad (5.6)$$

$$\text{For } (As \leq y/y_{50} \leq 6As) : p = 0.5p_u (y/y_{50})^{0.5} - 0.055p_u ((y - As(y_{50})) / (As(y_{50})))^{1.25} \quad (5.7)$$

$$\text{For } (6As \leq y/y_{50} \leq 18As) : p = 0.5p_u (6As)^{0.5} - 0.411p_u - 0.0625p_u (y/y_{50} - 6As) \quad (5.8)$$

$$\text{For } (y/y_{50} > 18As) : p = 0.5p_u (6As)^{0.5} - 0.411p_u - 0.75p_u As \quad (5.9)$$

8-Finally, the soil stiffness, E_{py} , is calculated as given by Equations (5.10) and (5.11) as: (API, 2000)

$$\text{For } (y/y_{50} \geq 10^{-6}) : E_{py} = p/y \quad (5.10)$$

$$\text{For } (y/y_{50} < 10^{-6}) : E_{py} = 0.25p_u ((10^{-6})^{0.5}) \quad (5.11)$$

5.2 Soil variability

Soil types and properties vary over a given space both vertically and horizontally. In soils, it is common to observe higher correlation in the horizontal direction than the vertical direction meaning that soil properties vary more rapidly in the vertical direction than the horizontal. Moreover, in addition to spatial variability, there is a point variability which arises as a result of uncertainty in estimating (measuring) the correct parameter in just one point.

Point and spatial variability of soil properties are commonly modeled using random fields (Fenton and Griffiths, 2008). This can be explained as; point variability is modeled with mean and covariance while spatial variability is modeled with spatial correlation.

In this study, the variability of undrained shear strength, S_u , is studied and Figure 5.2 shows variability of S_u with depth (spatial variable). A one-dimensional random field is implemented to simulate the variability of soil properties in the vertical direction while the soil properties in horizontal directions are assumed to be homogeneous. The random field which simulates the variability of S_u is defined as;

$$\{S'_u(z); z \in L \subset \mathbb{R}^d\} \sim h_{S_u}(S_u) \quad (5.12)$$

Where, $\{S'_u(z); z \in L\}$ is a realization of the random field, z is the reference variable $\{z \in L : 0 \leq z \leq 30\}$ or random field discretization ($z = z_1, \dots, z_n$), L is the reference domain, d is the dimensionality of the reference domain (e.g., $d = 1$; one-dimensional random field) and $h_{S_u}(S_u)$ is a probability density function (pdf) specifying the random field.

Figure 5.2 shows a random field realization of S_u , over 30m depth of stiff clay and the reference variable, z , is used to denote the random field discretization which divides L in to equal n -equal segments.

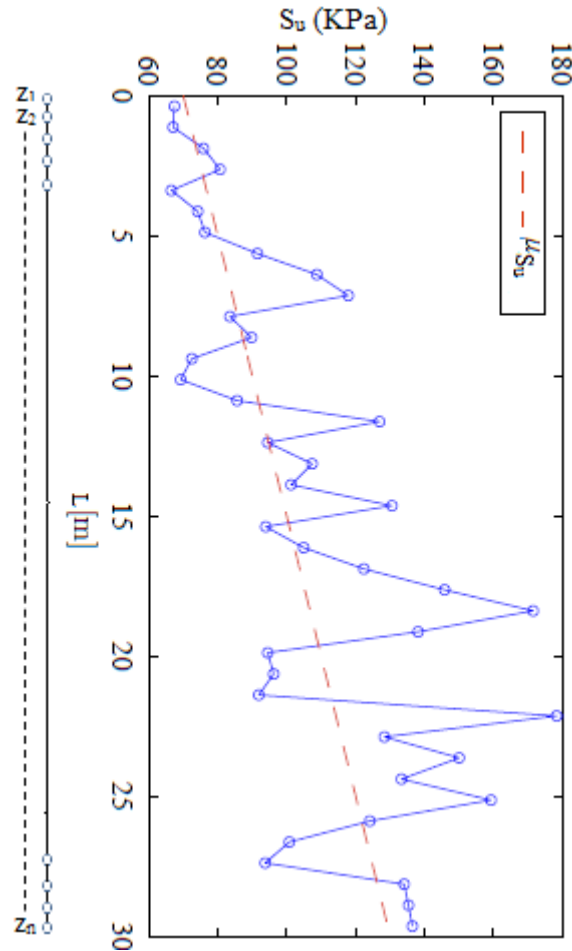


Figure 5.2 Shear strength over depth

The undrained shear strength is usually modelled as a lognormal distribution since the values are non-negative (Tang, 1995). Therefore, pdf $h_{S_u}(S_u)$ is defined as multivariate lognormal distribution by linearly increasing mean starting from $\mu_{S_u}=70$ at $z=0$ with an increment of 2. COV is equal to 0.25 while the spatial correlation is defined by the Markovian correlation function (exponential autocorrelation function) shown in Equation (5.14).

$$\mu_{S_u} = 70 + 2z \tag{5.13}$$

$$\rho_{\ln S_u}(z', z'') = \exp\left(-2\frac{\delta}{\phi}\right) \tag{5.14}$$

Where, $\delta=|z'-z''|$ is the distance between two points in the reference domain $\{z', z'' \in L \subset \mathbb{R}^1\}$ and ϕ is the correlation length which is defined, according to Fenton and Griffiths (2008), as

the distance within which the random properties are significantly correlated (e.g., $\phi = 2\text{m}$ in this study).

A common random field algorithm used to generate a Gaussian continuous random field is presented in Depina (2014) but this study is concerned with a lognormal distribution of S_u , therefore, some modifications have been implemented as shown below:

Algorithm for generating lognormal random fields

- Discretize the domain (L) into n segments: $z = (z_1, \dots, z_n)$, $n=30$ with each segment equal to 1m as can be seen in Figure 5.2.

- From the linear mean given by Equation (5.13), the lognormal mean and standard deviation are calculated using Equation (5.15)

$$\mu_{\ln S_u} = \ln \left(\frac{\mu_{S_u}^2}{\sqrt{\mu_{S_u}^2 + (\sigma_{S_u})^2}} \right) \text{ and } \sigma_{\ln S_u} = \sqrt{\ln \left(\frac{\sigma_{S_u}^2}{\mu_{S_u}^2} + 1 \right)} \quad (5.15)$$

- Calculate the n x n correlation matrix, **C**:

$$\mathbf{C} = \begin{bmatrix} \sigma_{\ln S_u}^2(z_1) & \dots & \dots & \dots & \sigma_{\ln S_u}(z_1)\sigma_{\ln S_u}(z_n)\rho_{\ln S_u}(z_1, z_n) \\ \sigma_{\ln S_u}(z_2)\sigma_{\ln S_u}(z_1)\rho_{\ln S_u}(z_2, z_1) & & & & \sigma_{\ln S_u}(z_2)\sigma_{\ln S_u}(z_n)\rho_{\ln S_u}(z_2, z_n) \\ \vdots & & \ddots & & \vdots \\ \sigma_{\ln S_u}(z_{n-1})\sigma_{\ln S_u}(z_1)\rho_{\ln S_u}(z_{n-1}, z_1) & & & & \sigma_{\ln S_u}(z_{n-1})\sigma_{\ln S_u}(z_n)\rho_{\ln S_u}(z_{n-1}, z_n) \\ \sigma_{\ln S_u}(z_n)\sigma_{\ln S_u}(z_1)\rho_{\ln S_u}(z_n, z_1) & \dots & \dots & \dots & \sigma_{\ln S_u}^2(z_n) \end{bmatrix} \quad (5.16)$$

- Decompose **C** in to a lower **A** and an upper **A^T** triangular matrix:

$$\mathbf{C} = \mathbf{A}\mathbf{A}^T \quad (5.17)$$

- Generate n x 1 vector of the standard normal distributed random values:

$$U_{S_u} \sim N(0,1) \quad (5.18)$$

- A Gaussian random field realization with mean $\mu_{\ln S_u}$ and **A** is calculated as:

$$S_u = \mu_{\ln S_u} + \mathbf{A}U \quad (5.19)$$

-A lognormal random field realization with mean $\mu_{\ln S_u}$ and **A** is calculated as:

$$S_u = \exp(\mu_{\ln S_u} + \mathbf{A}U) \quad (5.20)$$

Equation (5.20) gives the lognormal random field which simulates the uncertainties in the soil shear strength, S_u .

5.3 Lateral load

The monopile is laterally loaded with a random horizontal force H as a result of both wind and wave forces and a moment $M = H \cdot 30 \text{ m}$ applied at the sea bed level. The load is modeled by the Gumbel distribution (to simulate the extreme loading effect on the monopile resistance) with $\mu_H=2500\text{KN}$ and $\text{COV}_H=0.2$. (See Figure 5.3)

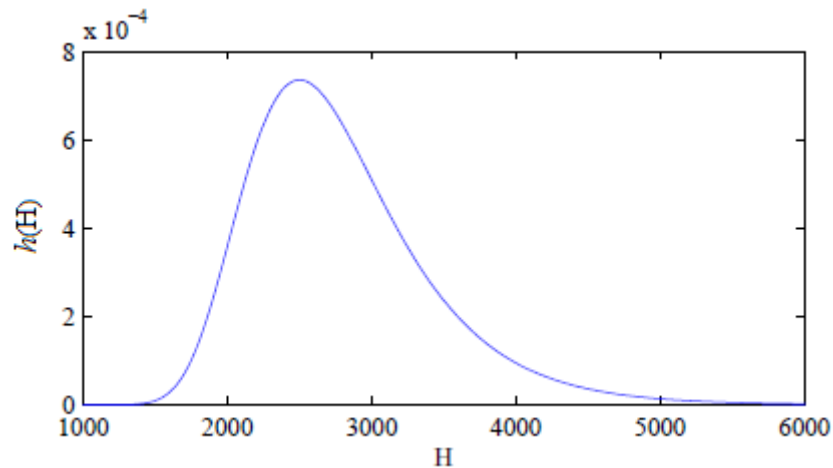


Figure 5.3 Gumbel distribution of lateral load, H

5.4 Pile geometry

The pile material is steel, modeled as a linear elastic with a Young’s modulus of $E_p = 210\text{MPa}$, a Poisson’s ratio of $\nu = 0.3$, moment of inertia, I_p and a unit weight of $\gamma_p = 78.35 \text{ KN/m}^3$.

$$\text{Moment of inertia} = I_p = \frac{\pi}{4} \left(\left(\frac{D}{2} \right)^4 - \left(\frac{D}{2} - w \right)^4 \right) \tag{5.21}$$

Various pile parameters (diameter, D , embedded length, L , and wall thickness, w) have been considered, as will be discuss in the next sections, to conduct the reliability-based design optimization of the monopile foundation.

5.5 Reliability analysis (Estimation of P_f for the monopile foundation)

The performance of monopile foundations is regulated by the serviceability limit state (SLS) and ultimate limit state (ULS). The SLS defines the state of the monopile where the deformations exceed the tolerance values while the load carrying capacity has not been surpassed. Specifically, the SLS is defined by a rotational limit (inclination) of the monopile at the sea bed level while the ultimate limit state (ULS) can be defined as an event where a

structure as a whole or some of its load bearing elements exceeded the load bearing capacity of the monopile (DNV, 2004 and API, 2000).

In this particular study, the CE method is implemented to estimate the probability of failure in which the load bearing capacity is exceeded (ULS); therefore, the reliability analysis is performed to analyze the effects of the uncertainties in S_u and H together with the pile parameters; D , w , L on the ULS. For a given combination of $\theta = [S_u, H]$ and $t = [D, w, L]$, the performance function is defined as the violation of the allowable (tolerable) stress given by Equations (5.22) and (5.23).

$$g(\theta, t) = \sigma_{lim} - \sigma(\theta, t) \tag{5.22}$$

$$\sigma(\theta, t) = \frac{M * D}{2 I_p} \tag{5.23}$$

Where

$\sigma_{lim} = 235\text{MPa}$ is the allowable yield stress of the monopile steel.

$\sigma(\theta, t)$ is the maximal stress in the monopile for diameter, D , moment of inertia, I_p , and moment, M (calculated using Equation (5.1b)).

5.5.1 Preparation of the Algorithm for Reliability

Procedures described in Algorithm 1.1 have been followed to develop the Cross-entropy algorithm to solve reliability or P_f .

1. Based on the findings in Chapter 4, $N=100$, $\rho=0.2$, $\alpha_r=1$ and $\beta_r=0.7$ have been selected and the iterator was set to $t=1$.
2. The performance function, $g(\theta, t)$, was calculated from the input parameters $\theta = [S_u, H]$ and $t = [D, w, L]$
 - The domain (L) has been discretized into n segments: $z = (z_1, \dots, z_n)$, where $n=30$ with each segment equal to 1m.
 - $U_{S_u} \sim N(0,1)$ has been generated as given by Equation (5.18) and transformed to S_u using Equation (5.20).
 - Similarly, $U_H \sim N(0,1)$ has been generated and transformed to H .
 - Moments along, $z = (z_1, \dots, z_n)$, the pile have been calculated using Equation (5.1b).
Note: p-y analysis discussed above is used to calculate the moments.
 - $\sigma(\theta, t)$ is calculated using Equation (5.23).

- Finally, $g(\boldsymbol{\theta}, \mathbf{t})$ was estimated.
3. Sort $g(\boldsymbol{\theta}, \mathbf{t})$ values in increasing order and denote the $\rho N+1$ quantile of the performance function by γ_t .
 4. All U_{Su} and U_H values which yield $g(\boldsymbol{\theta}, \mathbf{t}) \leq \gamma_t$ were identified and the weight has been calculated using Equation (3.9). The mean (μ_{Usu} and μ_{UH}) and standard deviation (σ_{Usu} and σ_{UH}) were calculated by solving Equation (3.11) and updated using Equations (3.17a) and (3.17b). The iterator was updated to $t = t+1$. Then, new normally distributed samples of U_{Su} and U_H with mean (μ_{Usu} and μ_{UH}) and standard deviation (σ_{Usu} and σ_{UH}) were generated with a sample size, N , as follow:

$$U = \mu_{Usu} + \text{randn}(\sigma_U) \quad (5.24)$$

$$UH = \mu_{UH} + \text{randn}(\sigma_{UH}) \quad (5.25)$$

5. U_{Su} and U_H were transformed to S_u and H respectively and the procedures stated in step 2 have been repeated.
6. If $g(\boldsymbol{\theta}, \mathbf{t}) \leq 0$, the probability of failure is calculated by Equation (3.14) as discussed in Chapter 3.

$$P_f = \frac{1}{N} \sum_{i=1}^N I(\theta_i) W(\theta_i; \mathbf{u}; \mathbf{v}_T) \quad (5.26)$$

5.6 Optimization Problem

RBDO problems are defined by Kupfer and Freudenthal (1977) as the minimizations of expected life time costs considering construction, maintenance costs and eventual failure.

Optimization is conducted in the discretized space Ω_t , such that the input parameters of the pile parameters are defined as $\mathbf{t} = [D, w, L] \subset \Omega_t$ and bounded such as $D \in [4.0, 4.1, \dots, 6.0]$, $w \in [0.02, 0.03, \dots, 0.1]$, and $L \in [25, 26, \dots, 40]$. The RBDO of the monopile foundation is then defined as:

$$\text{Minimize: } C(\boldsymbol{\theta}, \mathbf{t}) = C_i L \rho \pi \left[\left(\frac{D}{2} \right)^2 - \left(\frac{D}{2} - w \right)^2 \right] + C_F P_f(\boldsymbol{\theta}, \mathbf{t}) \quad (5.27a)$$

Subjected to

$$P_f(\boldsymbol{\theta}, \mathbf{t}) \leq P_f^{\text{tol}}, \quad (5.27b)$$

$$[4.0, 0.02, 25] \leq \mathbf{t} \leq [6.0, 0.1, 40] \quad (5.27c)$$

The cost of construction and installation is assumed to be $C_i(t)=2\text{€}/\text{kg}$ of the monopile with density of steel, $\rho=7835\text{kg}/\text{m}^3$, while the failure cost is estimated to be $C_F=10^7\text{€}$. For failure consequences associated with offshore wind turbines, $P_f^{\text{tol}}=10^{-4}$ is selected.

5.6.1 Preparation of the Algorithm for Optimization

Procedures described in Algorithm 2.1 have been followed to implement the CE algorithm to solve the optimization with the objective function given by Equation (5.27a).

- 1- From the important findings of Chapter 4; $N=100$, $\rho=0.1$, $\alpha_p=0.98$ and $\beta_p=0.98$ have been selected and the iterator was set to $t=1$.
- 2- N bounded random numbers have been generated such as $D \in [4.0, 4.1, \dots, 6.0]$, $w \in [0.02, 0.03, \dots, 0.1]$, and $L \in [25, 26, \dots, 40]$.
- 3- Using each set of the randomly generated numbers, $\mathbf{t}_i=[D_i, w_i, L_i]$, the probability of failure, P_f , was calculated as discussed in Section 5.5.1 or Algorithm 1.1; therefore, for the values which satisfy the reliability constraint, the final cost is calculated using Equation (5.27a).
- 4- $C(\mathbf{0}, \mathbf{t}_i)$ values were sorted in increasing order and denoted the $\rho N+1$ quantile of the performance function by γ_t .
- 5- All \mathbf{t}_i values which yield $C(\mathbf{0}, \mathbf{t}_i) \leq \gamma_t$ were identified using weight, $W=1$, Equation (3.16) was solved to get the respective vector of mean, $[\mu_D, \mu_w, \mu_L]$ and standard deviation, $[\sigma_D, \sigma_w, \sigma_L]$ and then updated using Equations (3.17a) and (3.17b).
- 6- Then, new normally distributed samples $\mathbf{t}_i=[D_i, w_i, L_i]$ based on mean, $[\mu_D, \mu_w, \mu_L]$ and standard deviation, $[\sigma_D, \sigma_w, \sigma_L]$ were generated with a sample size, N . In each case the generated values were checked if it is within the bounds as given by Equation (5.27c).

$$D \sim N(\mu_D, \sigma_D) \tag{5.28}$$

$$w \sim N(\mu_w, \sigma_w) \tag{5.29}$$

$$L \sim N(\mu_L, \sigma_L) \tag{5.30}$$

- 7- The procedures starting from step 2 were repeated until the mean values converge or the standard deviations were close to zero.
- 8- The mean, $[\mu_D, \mu_w, \mu_L]$, at the last iteration are taken as the optimal monopile design parameters and the corresponding cost is the design cost of the monopile.

5.7 Results and Discussion

The estimation of the probability of failure for the laterally loaded monopile foundation was started by studying the effects of α_r and β_r of the CE method on the estimates of the failure probabilities and the results were compared with the result of Subset simulation (SS).

For optimization analysis, the results obtained by implementing the CE algorithm are compared with Simulated annealing and compared in terms of efficiency and accuracy.

Section 5.7.1 presents the results and discussion for the reliability analysis while the optimization analysis results are summarized in Section 5.7.2.

5.7.1 Reliability Analysis of a monopile foundation

The discussion in Chapter 4 recommended the use of $N \geq 100$ and $\rho > 0.1$ to estimate P_f for high dimensional problems. Therefore, $N=100$ and $\rho=0.2$ have been chosen for this case to study the effects of the updating parameters. Moreover, the parameters $D=5m$, $w=0.05m$ and $L=30m$ have been selected within the allowable range for the monopile parameters (Equation (27.c)).

Similar to the discussion in Chapter 4, the study on α_r and β_r showed that the choice of α_r does not have a significant effect on the final result while β_r between 0.5 and 1 leads to accurate estimate. As β_r approaches to 1, the calculation was time consuming (high number of iteration) because of less convergence of the standard deviation to zero. In general, it can be observed from Table 5-3, the P_f values are less than 10^{-4} which shows the capability of the CE method in estimating rare-events.

Table 5-3 Estimation of P_f for the different combinations of α_r and β_r

α_r	β_r	Iteration, T	P_f
1	0.5	6	1,854e-06
1	0.7	6	6,043e-06
1	1	8	1,223e-06

Table 5-4 shows the effect of ρ , on P_f for $\alpha_r= 1$, $\beta_r= 0.7$ and $N=100$. Each case was run 10 times and it was observed the estimate of P_f yielded a value between $7.800e-06$ and $3.500e-05$ so Table 5-4 shows the average values obtained. The discussion on Chapter 4 recommended the use of $\rho > 0.1$ for high dimensional problems and similarly in this case, $\rho = 0.1$ resulted in time consuming computation and instability in P_f estimations. The use of $\rho = 0.2$ and 0.3 resulted similar estimate of P_f though more consistent results were obtained for $\rho = 0.3$.

Table 5-4 Effect of ρ on estimate of P_f

CE			
ρ	Iteration, T	Time (minutes)	P_f
0.2	6	6	7.800e-06
0.3	5	8	7.697e-06

5.7.1.1 Comparison of the CE method with subset simulation

The study on the monopile foundation is extended further to compare the results obtained based on the CE algorithm with SS method in terms of efficiency and accuracy. Two cases have been considered:

Case-1) Comparison of the CE (using $N=100$, $\rho = 0.2$ and $N=300$, $\rho = 0.3$) with SS (using $N=100$ and $\rho = 0.1$) for the monopile foundation with parameters; $D=5m$, $w=0.05m$ and $L=30m$.

Table 5-5 shows the results of 15 simulations of the CE and SS for Case-1 and the number of iterations (T), time of simulation and P_f are also presented. The consistency in estimating P_f was found to be better in the CE method than SS in which most results were concentrated in the border between 10^{-5} and 10^{-6} while for the SS method there was some discrepancy which range between 10^{-4} and 10^{-7} . Moreover, the consistency of the result was improved by increasing the sample size from 100 to 300 although the computation became more intensive (time consuming).

Table 5-5 Comparison of CE with SS for monopile foundation, Case-1

CE (N=100, $\rho = 0.2$)			CE (N=300, $\rho = 0.3$)			SS (N=100, $\rho = 0.1$)		
T	Time (minute)	P_f	T	Time (minute)	P_f	T	Time (minute)	P_f
4	6	1.86e-05	4	8	4.52e-05	6	7	2.66e-06
5	3	3.87e-06	6	11	4.81e-06	4	5	6.00e-05
6	7	1.82e-06	4	11	3.82e-06	5	7	1.00e-06
4	6	4.19e-05	4	12	1.09e-05	6	7	4.90e-06
7	8	1.36e-06	4	11	7.92e-06	4	5	2.70e-05
6	7	2.34e-06	4	11	6.31e-06	6	8	7.40e-06
5	6	1.54e-05	4	10	5.54e-06	5	6	2.60e-06
5	4	3.87e-06	4	11	3.87e-06	6	7	1.30e-06
6	3	4.50e-06	4	9	8.36e-06	5	7	3.90e-06
5	6	2.29e-06	4	11	2.29e-06	6	7	2.40e-07
5	6	4.36e-06	4	12	1.36e-05	5	8	1.30e-05
5	6	7.31e-06	5	11	6.23e-06	6	8	2.10e-06
5	6	3.11e-05	4	12	3.11e-06	6	7	4.30e-06
5	7	3.00e-06	4	11	8.12e-06	5	6	4.30e-07
5	6	3.11e-06	4	11	3.11e-06	5	6	4.30e-06

In Table 5.5, 15 simulation results for Case-1 were presented and Table 5.6 summarizes the results as a mean and covariance of P_f . Moreover, the average time of simulation and the number of iterations (T) are presented. The mean values of P_f obtained by the CE agree well with the estimate of P_f using SS. The comparison based on the covariance and time of simulation show that the CE gave more consistent estimate of P_f in a relatively less time of simulation.

Table 5-6 Summary of comparison between CE and SS methods

Method		CE (N=100, $\rho = 0.1$)	CE (N=300, $\rho = 0.3$)	SS (N=100, $\rho = 0.1$)
P_f	Mean, μ	9.653e-06	8.881e-06	9.008e-06
	COV	1.26	1.18	1.74
T	Average	5	4	5
Time (minute)	Average	6	11	7

Case-2) Comparison of the CE (using N=100, $\rho = 0.2$) with Subset simulation for a random monopile foundation parameters ($4 \leq D \leq 6$, $0.01 \leq w \leq 0.1$ and $25 \leq L \leq 40$).

The simulations results for Case-2 are presented in Table 5-7. Each simulation was run three times and the results displayed in the table are the average values.

Table 5-7 shows the estimate of P_f obtained by implementing the Cross-entropy method gave similar result (accuracy) and number of iteration (efficiency) with the SS method. The values of probability of failure vary for the different combinations of D, w and L. For example, D=4m, w=0.02m and L=20m gave highest probability of failure in Table 5-7.

Table 5-7 Comparison with SS for random pile dimensions (D, w and L)

D (m)	w (m)	L (m)	CE		SS	
			P_f	Iteration	P_f	Iteration
4	0.02	20	1	1	1	1
4.50	0.06	35	3.3989e-06	6	6.7.6e-06	6
5.2	0.08	40	<1.00e-8	>8	<1.00e-8	>8
5.4	0.02	28	0.0117	2	0.058	2
5.6	0.08	34	<1.00e-8	>8	<1.00e-8	>8
5.6	0.02	40	0.02	2	0.01	3
5.8	0.04	28	2,7226e-06	4	2.6e-06	4
5.80	0.02	20	0.0144	2	0.01	2
6	0.05	30	<1.00e-8	>8	<1.00e-8	>8
6	0.08	40	<1.00e-8	>8	<1.00e-8	>8

5.7.2 Results for the Optimization Problem

The simulation of the optimization sub-problem within the RBDO problem was time consuming and in average it took five days for each simulation. Three simulations were run to get the optimum monopile parameters (D , w , L) which yield the minimum (design) cost (C_{min}). The results obtained using the CE algorithm and Simulated annealing are presented in Table 5-8.

Table 5-8 Pile Parameters D , w , L with initial cost C_i and minimum final cost C_{min}

Method	Simulation	Final Cost (C_{min} , €)	D (m)	w (m)	L (m)	P_f	Initial Cost (C_i , €)
<i>CE (cross-entropy)</i>	1	3.1372e+05	5.70	0.045	25	8.500e-5	3.1286e+05
	2	3.2490e+05	5.15	0.045	30	4.600e-5	3.2481e+05
	3	3.0268e+05	5.95	0.035	29	5.200e-5	2.9998e+05
<i>Simulated Annealing</i>		3.0021e+05	5.20	0.04	29	6.400e-5	2.9880e+05

The results on Table 5-8 shows the initial cost and design (optimum) cost obtained using the Cross-entropy method agree well with the robust Simulated annealing optimization method.

The optimum results D , w and L are the mean values obtained after four iterations. The stopping criterion for the CE algorithm was set so that the standard deviation for the wall thickness of the pile, w , is less than 10^{-4} so that D converged with in three decimal places and L converged to two decimal places as can be seen in Table 5-9.

Table 5-9 Convergence of D , w and L as a result of small standards deviation

standard deviation	Iteration			
	1	2	3	4
σ_D	0.1190	0.0267	0.0059	0.00163
σ_w	0.0029	0.0006	0.0001	4.00e-05
σ_L	1.3651	0.2667	0.0831	0.0229

The three simulation results using the CE method have already presented in Table 5-8. The optimum monopile parameters for Simulation 2 were obtained to be $D=5.15m$, $w=0.045m$, $L=30$ and the minimum cost, $C_{min}= 3.2490e+05€$. Therefore, the next portion illustrates how the optimum monopile dimensions and the design cost have been obtained.

Figure 5.4 illustrates how the optimum diameter of the monopile was attained. The diameter was initially bounded between 4m and 6m and under the implementation of the CE algorithm on optimization problem it converged to $D=5.15m$ after four iterations.

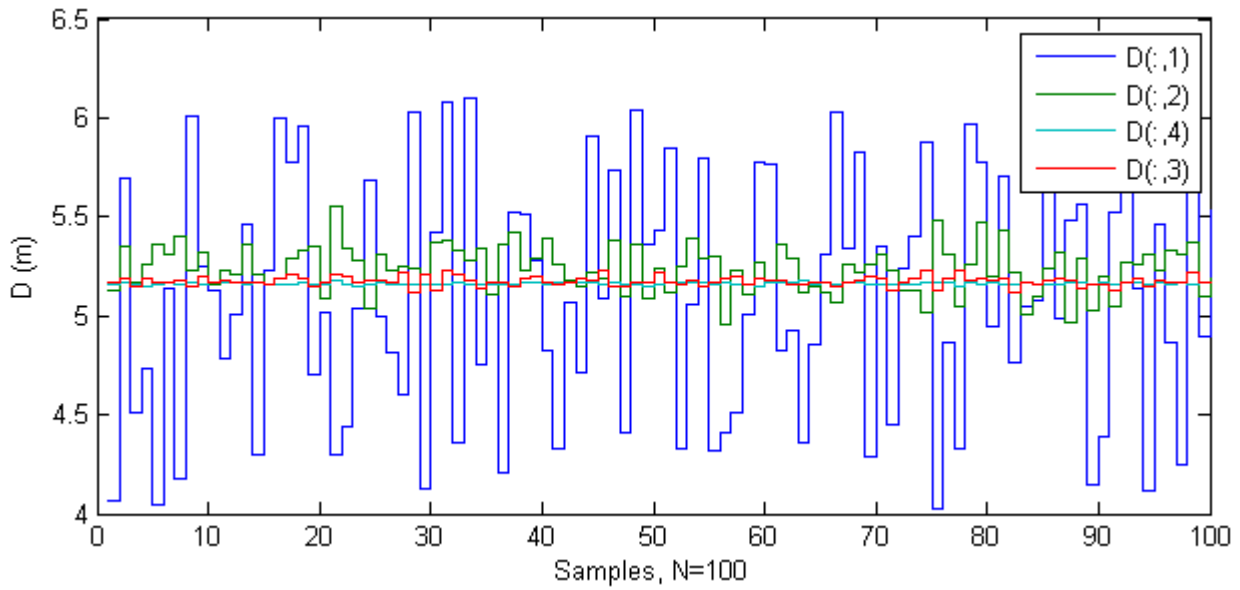


Figure 5.4 Evolution of D to optimum value, $D=5.15m$, after four iterations

Similarly, Figure 5.5 illustrates how the optimum embedment depth of the monopile was attained. L was initially bounded between 25m and 40m. The evolution of L from the initial bounded limit to the optimum under the CE algorithm resulted in $L=30m$ after four iterations.

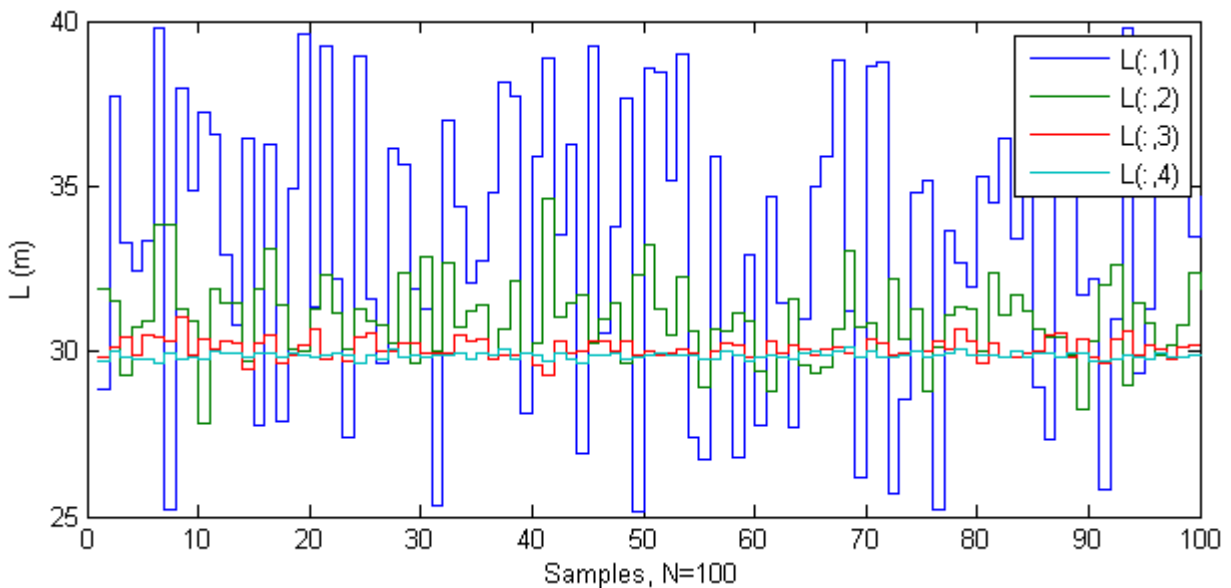


Figure 5.5 Evolution of L to optimum value, $L=30m$, after four iterations

The wall thickness, w , plot on Figure 5.6 shows the convergence of w to the optimum, $w=0.045m$ after four iterations. From Table 5-9, it was shown that the standard deviation after four iterations was $\sigma_w = 4.00e-05$ for $N=100$ samples which shows an accurate convergence of w to 0.045m.

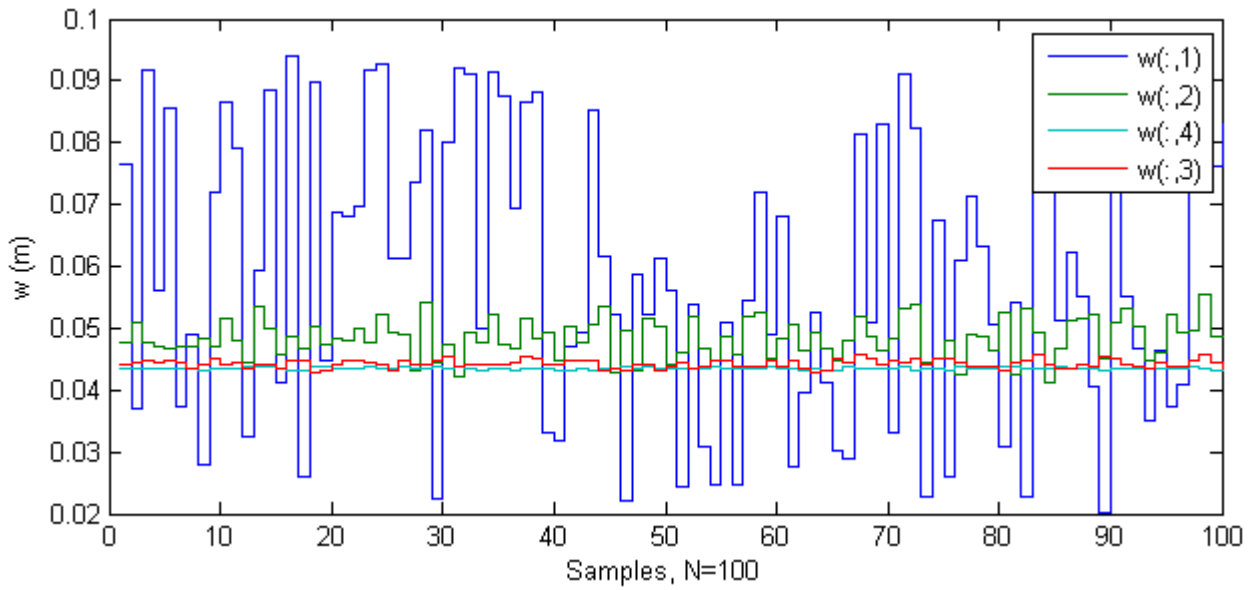


Figure 5.6 Evolution of w to optimum value, $w=0.045m$, after four iterations

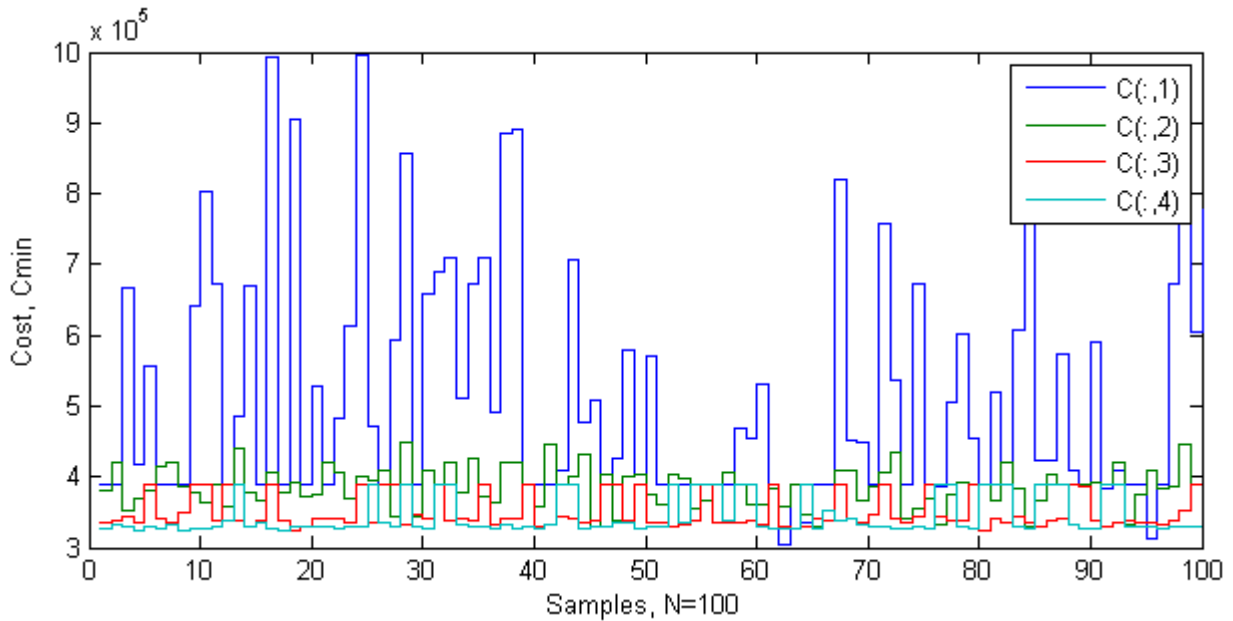


Figure 5.7 Evolution of cost to optimum value, $C_{min} = 3.2490e+05€$, after four iterations

So far, Figures 5.4, 5.5 and 5.6 illustrated convergence to the optimum monopile parameters D , w and L . Figure 5.7 shows the evolution of the estimated costs to the design (minimum) cost at each iteration. The convergence to design cost was obtained after four iterations to be $C_{min} = 3.2490e+05€$.

As a conclusion, the above discussion and Table 5-8 show the estimated design cost by implementing the CE algorithm agrees well with the robust simulated annealing optimization method.

6. Summary and Conclusions

6.1 Introduction

The main task for this thesis was to implement the Cross-entropy method to solve independently reliability and optimization sub-problems within the RBDO problem. The performance of the Cross-entropy method was examined on an RBDO problem with an analytical solution and a practical problem of a monopile foundation for offshore wind turbine. The investigation on the performance of the Cross-entropy method with respect to accuracy and efficiency on both reliability and optimization problems as compared to several commonly used methods was also the main interest to be evaluated.

A numerical approach has been utilized as the basic study methodology. Preparation of the algorithms to solve both reliability and optimization problems was done by implementing and coding on the high level language of MATLAB (version R2014a and R2013b), developed by MathWorks company.

The summary of important findings, conclusion, recommendations and possible future works are presented in this chapter.

6.2 Summary of Important findings

The implementation and evaluation of the CE algorithm was performed initially on a RBDO problem with an analytical solution. Then, the CE algorithm was implemented further on a RBDO problem of a laterally loaded monopile foundation of offshore wind turbine. Some important and interesting findings have been observed by conducting this particular study. These basic findings are presented in the next sections, divided in-to reliability (Section 6.2.1) and optimizations findings (Section 6.2.2).

6.2.1 Summary on reliability analysis and findings

Algorithm 1.1 was initially implemented for reliability analysis to estimate P_f on one-dimensional problem (1D). The implementation of the CE algorithm was then extended to two-dimensional (2D) and even up to hundred dimensional (100D) problems. Parallel to the implementation of the algorithm, the study on the effects of the updating parameters (α_r and β_r), percentage of failure at each iteration (ρ), and number of samples (N) were evaluated. The developed algorithm was first tested on a problem within an analytical solution and finally applied on a monopile foundation design; therefore, the important findings can be presented on the following two categories.

6.2.1.1 Important findings based on a problem that has analytical solution

-For a one-dimensional ($n=1$ and $d=1$) problem, the CE method gave a better estimate of probability of failure as compared to the existing methods such as Monte Carlo (MC) and Importance sampling (IM). Moreover, the CE method required less computational time and required less sample size as compared to MC and IM methods. Therefore, the method was found to be both accurate and efficient.

-For two-dimensional ($n=2$ and $d=2$) problems, the CE method resulted in good estimation of P_f and required less computational time (efficient) as compared to both MC and SS methods.

-For problems with $2 < n < 10$ and $2 < d < 10$, the study on the updating parameters α_r and β_r showed that the choice of α_r does not have a significant effect on the final result while β_r between 0.5 and 1 leads to an accurate estimate; therefore, $\alpha_r=1$ and $\beta_r=0.7$ have been selected on this particular study. Moreover, the study on N and ρ showed the use of $N=100$ and $\rho=0.1$ were found sufficient to give good estimates of P_f and required less computational time than higher N and ρ .

-For problems with $n=(10-20)$ and $d=(10-20)$, increase in N was required, and change from $N=100$ to 1500 resulted in a more accurate estimate of P_f .

-For problems with $n=(20-60)$ and $d=(20-60)$, the use of $\rho=0.1$ did not yield accurate estimates; therefore, it was increased to $\rho=0.4$ and together with $N=1500$ gave good estimate of P_f .

-For problems with $n > 60$ and $d > 60$, the method did not yield stable estimates. This may demonstrate the limit of the CE method.

6.2.1.2 Important findings based on monopile foundation design

-For a given monopile foundation parameters $D=5\text{m}$, $w=0.05\text{m}$ and $L=30\text{m}$, the choice of α_r did not show significant effect on the estimation of P_f while β_r between 0.5 and 1 leads to an accurate estimate. As β_r approaches to 1, the calculation was found to be time consuming; therefore, as discussed earlier on Section 6.2.1.1, $\alpha_r=1$ and $\beta_r=0.7$ were chosen, and the results based on the CE method agree well with the Subset simulation estimates of P_f .

-The number of iterations and time required for a simulation has been slightly less for the CE than SS (Subset simulation) for the same N and ρ .

-The consistency of the results, which is based on the covariance calculation of P_f estimates, was found to be better in the CE than SS method.

6.2.2 Summary on Optimization analysis and findings

The study on optimization problems concentrated to minimize the final cost for a given objective function. RBDO problems are commonly defined as minimizations of expected life time costs considering construction, maintenance costs and eventual failure (Kupfer and Freudenthal, 1977); therefore, the reliability analysis method discussed earlier or Algorithm 1.1 was used to estimate failure probability, and the procedures given by Algorithm 2.1 were followed to solve the optimization problems.

Similar to the reliability analysis problems presented earlier, the implementation of the CE method on optimization problems was initially performed on a problem which has an analytical solution. Then, the method was implemented on a monopile foundation design to estimate the monopile parameters D , w , and L that yield the minimum (design) cost; therefore, the important findings observed are presented next.

6.2.2.1 Important findings based on a problem that has an analytical solution

-For two-dimensional ($n=2$ and $d=2$) problems, the use of sample sizes 200, 500 and 2000 resulted in good estimates of the final cost approximate to the analytical (true) solution.

-The study on the updating parameters showed that change in α_p does not significantly affect the final result of the minimum cost while it was observed during simulation that the choice of β_p can significantly affect the accuracy and efficiency of the approach.

-For higher dimensions ($n \leq 20$ and $d \leq 20$), the reliability analysis required large sample size, N , and $\rho > 0.1$. Therefore, the parameters $\alpha_r=1$, $\beta_r=0.7$, $N=500$ and $\rho=0.2$ were used for estimation of P_f (using Algorithm 1.1) while $\alpha_p=0.98$, $\beta_p=0.98$, $N=100$ and $\rho=0.1$ were used

for optimization of the minimum cost (using Algorithm 2.1) to yield good estimate of the final cost.

-For $n=30$ and $d=30$, the estimate of the final cost based on the CE method gave considerably lower than the true estimate although $N=1500$ and $\rho=0.4$ were used. This may be because the algorithm cannot simulate the high dimensional problem showing the limit of the CE method.

6.2.2.2 Important findings based on a monopile foundation

-The implementation of the CE algorithm on a monopile foundation RBDO problem yielded the optimum monopile dimensions (D , w and L) and the respective final design cost (minimum cost). The final design cost obtained using the CE algorithm was compared to an existing optimization method (Simulated annealing) and showed good agreement.

-Since the RBDO for the monopile foundation features only three optimization variables (D , w and L), the CE-RBDO performed well; therefore, $\alpha_p=0.98$, $\beta_p=0.98$, $N=100$ and $\rho=0.2$ have been found to be enough to give estimate of the minimum cost.

6.3 Conclusion, Recommendations and Future works

6.3.1 Conclusion and Recommendations

The aim of this thesis is to implement the Cross-entropy method for reliability-based design optimization (RBDO). The CE method showed efficient performance on RBDO problems with analytical solutions and a monopile foundation design of offshore wind turbines. Moreover, the method showed efficient and accurate result by comparing it to analytical solutions and existing reliability as well as optimization methods.

The CE method showed limitations in the dimensionality of both reliability and optimization problems. Special attention should be given to parameter selection so that the important findings on α , β , ρ and N from this study can be used as a preliminary input for similar problems but it is recommended to study the effects of the parameters by changing the values.

Finally, the main merit and beauty of the CE method can be summed as the ability and flexibility to solve both reliability and optimization problems which makes the method suitable to solve RBDO problems; therefore, the implementation of CE to solve RBDO problems saves time rather than the use of two different methods to solve the reliability and optimization sub-problems within the RBDO respectively.

6.3.2 Future works

The efficiency and accuracy of the cross-entropy method can be modified:

- The CE method showed limitations in the dimensionality of both reliability and optimization problems for the academic problem considered. It gave accurate estimates of probability of failure for dimensionality or input parameters $d < 60$ while it gave estimates of the minimum cost up to 30 input parameters. The study can extend to investigate and evaluate on the limits of the CE method to account for more dimensional.
- It is recommended to give special attention for the parameter selection (α , β , ρ and N) because the final output may be affected by the values of the parameters. Detailed parameter analysis study can be conducted that may enhance the efficiency of the method.

References

- AARST, E. & KORST, J. 1989. Simulated Annealing and Boltzmann Machines-A Stochastic Approach to Combinatorial Optimization and Neural Computers. New York: Wiley.
- ALON, G., KROESE, D. P., RAVIV, T. & RUBINSTEIN, R. Y. 2005. Application of the cross-entropy method to the buffer allocation problem in a simulation-based environment. *Annals of Operations Research*, 134, 137-151.
- AOUES, Y. & CHATEAUNEUF, A. 2010. Benchmark study of numerical methods for reliability-based design optimization. *Structural and Multidisciplinary Optimization*, 41, 277-294.
- AU, S.-K. & BECK, J. L. 2001. Estimation of small failure probabilities in high dimensions by subset simulation. *Probabilistic Engineering Mechanics*, 16, 263-277.
- AU, S. 2005. Reliability-based design sensitivity by efficient simulation. *Computers & structures*, 83, 1048-1061.
- AU, S. & BECK, J. L. 1999. A new adaptive importance sampling scheme for reliability calculations. *Structural Safety*, 21, 135-158.
- BEASLEY, D., MARTIN, R. & BULL, D. 1993. An overview of genetic algorithms: Part 1. Fundamentals. *University computing*, 15, 58-58.
- BEKKEN, L. 2009. *Lateral behavior of large diameter offshore monopile foundations for wind turbines*. TU Delft, Delft University of Technology.
- BOTEV, Z. I., KROESE, D. P., RUBINSTEIN, R. Y. & L'ECUYER, P. 2013. The cross-entropy method for optimization. *Machine Learning: Theory and Applications*, V. Govindaraju and CR Rao, Eds, Chennai: Elsevier BV, 31, 35-59.
- BUSONI, L., BABUSKA, R., DE SCHUTTER, B. & ERNST, D. 2010. *Reinforcement learning and dynamic programming using function approximators*, CRC press.
- CHEPURI, K. & HOMEM-DE-MELLO, T. 2005. Solving the vehicle routing problem with stochastic demands using the cross-entropy method. *Annals of Operations Research*, 134, 153-181.
- CHOI, S.-K., GRANDHI, R. & CANFIELD, R. A. 2006. *Reliability-based structural design*, Springer Science & Business Media.
- COHEN, I., GOLANY, B. & SHTUB, A. 2005. Managing stochastic, finite capacity, multi-project systems through the cross-entropy methodology. *Annals of Operations Research*, 134, 183-199.
- DE BOER, P.-T., KROESE, D. P., MANNOR, S. & RUBINSTEIN, R. Y. 2005. A tutorial on the cross-entropy method. *Annals of operations research*, 134, 19-67.
- DE BOER, P., KROESE, D. P. & RUBINSTEIN, R. Y. 2004. A fast cross-entropy method for estimating buffer overflows in queueing networks. *Management Science*, 50, 883-895.
- DEPINA, I. 2014. Lecture Note for Geohazards and Risk Assessment. NTNU (Norwegian University of Science and Technology).
- DEPINA, I., LE, T. M. H., EIKSUND, G. & BENZ, T. 2015. Behavior of cyclically loaded monopile foundations for offshore wind turbines in heterogeneous sands. *Computers and Geotechnics*, 65, 266-277.

- DU, X. & CHEN, W. 2004. Sequential optimization and reliability assessment method for efficient probabilistic design. *Journal of Mechanical Design*, 126, 225-233.
- DUBOURG, V., SUDRET, B. & BOURINET, J.-M. 2011. Reliability-based design optimization using kriging surrogates and subset simulation. *Structural and Multidisciplinary Optimization*, 44, 673-690.
- ELISHAKOFF, I., VAN MANEN, S. & ARBOCZ, J. 1987. First-order second-moment analysis of the buckling of shells with random imperfections. *AIAA journal*, 25, 1113-1117.
- ENEVOLDSEN, I. & SØRENSEN, J. D. 1994. Reliability-based optimization in structural engineering. *Structural safety*, 15, 169-196.
- FENTON, G. A. & GRIFFITHS, D. V. 2008. *Frontmatter*, Wiley Online Library.
- FISSLER, B., RACKWITZ, R. & NEUMANN, H.-J. 1979. Quadratic limit states in structural reliability. *Journal of the Engineering Mechanics Division*, 105, 661-676.
- FREUDENTHAL, A. M. 1956. Safety and the probability of structural failure. *American Society of Civil Engineers Transactions*, 121, 1337-1397.
- GILKS, W. R. 2005. *Markov chain monte carlo*, Wiley Online Library.
- GOFFE, W. L., FERRIER, G. D. & ROGERS, J. 1994. Global optimization of statistical functions with simulated annealing. *Journal of Econometrics*, 60, 65-99.
- GOLDBERG, D. E. & HOLLAND, J. H. 1988. Genetic algorithms and machine learning. *Machine learning*, 3, 95-99.
- GU, Q. 2014. Performance and Risk Assessment of Soil-Structure Interaction Systems Based on Finite Element Reliability Methods. *Mathematical Problems in Engineering*, 2014, 5.
- HASOFER, A. M. & LIND, N. C. 1974. Exact and invariant second-moment code format. *Journal of the Engineering Mechanics division*, 100, 111-121.
- KEITH, J. & KROESE, D. P. Rare event simulation and combinatorial optimization using cross entropy: sequence alignment by rare event simulation. Proceedings of the 34th conference on Winter simulation: exploring new frontiers, 2002. Winter Simulation Conference, 320-327.
- KOTHARI, R. P. & KROESE, D. P. Optimal generation expansion planning via the cross-entropy method. Winter Simulation Conference, 2009. Winter Simulation Conference, 1482-1491.
- KROESE, D. P., HUI, K.-P. & NARIAI, S. 2007. Network reliability optimization via the cross-entropy method. *Reliability, IEEE Transactions on*, 56, 275-287.
- KUPFER, H. & FREUDENTHAL, A. Structural optimization and risk control. Proceedings of the 2nd International Conference on Structural Safety and Reliability (ICOSSAR'77), 1977. Munich, Germany, 627-639.
- LEBLANC, C. 2009. *Design of offshore wind turbine support structures*. Department of Civil Engineering, Aalborg University, Denmark.
- PHOON, K.-K. 2008. *Reliability-based design in geotechnical engineering: computations and applications*, CRC Press.
- ROYSET, J. O., DER KIUREGHIAN, A. & POLAK, E. 2001. Reliability-based optimal structural design by the decoupling approach. *Reliability Engineering & System Safety*, 73, 213-221.

- RP2A-WSD, A. Recommended practice for planning, designing and constructing fixed offshore platforms—working stress design—. Twenty-, 2000.
- RUBINSTEIN, R. 1999. The cross-entropy method for combinatorial and continuous optimization. *Methodology and computing in applied probability*, 1, 127-190.
- RUBINSTEIN, R. Y. 1997. Optimization of computer simulation models with rare events. *European Journal of Operational Research*, 99, 89-112.
- RUBINSTEIN, R. Y. 2001. Combinatorial optimization, cross-entropy, ants and rare events. *Stochastic optimization: algorithms and applications*. Springer.
- SCHRAUDOLPH, N. N. 1995. *Optimization of entropy with neural networks*. Citeseer.
- SCHUËLLER, G., PRADLWARTER, H. & KOUTSOURELAKIS, P. 2004. A critical appraisal of reliability estimation procedures for high dimensions. *Probabilistic Engineering Mechanics*, 19, 463-474.
- SCHUËLLER, G. I. & STIX, R. 1987. A critical appraisal of methods to determine failure probabilities. *Structural Safety*, 4, 293-309.
- TAFLANIDIS, A. & BECK, J. 2008. Stochastic subset optimization for optimal reliability problems. *Probabilistic Engineering Mechanics*, 23, 324-338.
- TANG, W. H., ENGINEERING, N. R. C. C. O. R. M. F. R. M. I. G., BOARD, N. R. C. G., ENERGY, N. R. C. B. O., SYSTEMS, E., ENGINEERING, N. R. C. C. O. & SYSTEMS, T. 1995. *Probabilistic Methods in Geotechnical Engineering*, National Academies.
- TICHÝ, M. 1994. First-order third-moment reliability method. *Structural Safety*, 16, 189-200.
- TU, J., CHOI, K. K. & PARK, Y. H. 2001. Design potential method for robust system parameter design. *AIAA journal*, 39, 667-677.
- VALDEBENITO, M. A. & SCHUËLLER, G. I. 2010. A survey on approaches for reliability-based optimization. *Structural and Multidisciplinary Optimization*, 42, 645-663.
- VEITAS, D. N. 2004. *Design of offshore wind turbine structures*, Det Norske Veritas.
- WONG, H. 1996. *Genetic Algorithms* [Online]. Available: http://www.doc.ic.ac.uk/~nd/surprise_96/journal/vol1/hmw/article1.html [Accessed March 10 at 2:20 2014].